

## System Simulation of Array-Fed Satellite Reflector Antennas

**Lishuai Jing**

*Signal Processing Group*

*Department of Signals and Systems*

Chalmers University of Technology

*Göteborg, Sweden, 2010*

*EX035/2010*

# CHALMERS



## **System Simulation of Array-Fed Satellite Reflector Antennas**

**Lishuai Jing**

*Signal Processing Group*

*Department of Signals and Systems*

**Chalmers University of Technology**

*Göteborg, Sweden, 2010*

Supervisors at RUAG Space:

Per Magnusson, (Title)

Per Ingvarson, (Title)

Examiners at Chalmers:

Mats Viberg, Professor

Per Jacobsson, Post Doctor

# Abstract

Satellite mobile communication has attracted a lot of attention in the last decades. Large reflector antennas (10-20m) with an array of a few hundred feed radiators are employed in such systems. This is also known as array fed reflector antenna systems. The radiators are at L or S-band<sup>1</sup> with combining of the receive and transmit functions. A diplexer is used to separate receive from transmit.

In this thesis, a multi-beam antenna (MBA) satellite communication system with high beam gain and frequency reuse capability is modelled in Matlab. A simple model which demonstrates the beamforming algorithms is modelled in Simulink as well. In the system simulation, beam overlap is achieved by employing a beamforming network. Flexible power sharing and even traffic distribution between different beams are accomplished by using the Butler Matrix Power Amplifiers (BMPAs). Each BMPA contains two Butler matrixes that connect back to back with High Power Amplifiers (HPAs) in between. One Butler matrix is used to even the power load for the HPAs and the other one is used for routing the signal to the desired output port. Identical 4 by 4 Butler matrixes are used to reduce the mass, insertion loss and increase the flexibility of the transmit system as compared to a single large Butler matrix.

A geostationary (GEO) satellite with a focal array which has 42 antenna elements is our focus. The transmit system performance is measured by evaluating the gain variations on each beam coverage edge and investigating the side lobe levels (SLL) of the same frequency beams. The receive system is measured by the noise performance. The mutual coupling effect between the antenna elements could be measured as well. The transmit and receive systems are combined with diplexers and the isolation level is defined. The system model can be easily extended to a much larger array by using the same concept as described in this thesis.

**Keywords:** Satellite mobile communication, Array fed reflector antenna system, System modelling, Beamforming network

---

<sup>1</sup> In terms of the L and S band, we refer to around 1500 MHz and 2100 MHz, respectively.

# Acknowledgements

This thesis is performed in collaboration with RUAG Space and Chalmers University of Technology. It was developed from January 2010 to June 2010 at the antenna group of RUAG Space, Sweden.

Firstly, I would like to thank Per Ingvarson and Per Magnusson for providing such a precious opportunity for me to perform this challenging and interesting thesis at RUAG Space. Their experienced guidance, effortless explanations, scientific attitude and well organized working process will be a great treasure for my future career. In addition, I would like to express my gratitude to professor Mats Viberg and Dr. Per Jacobsson at the Signal Processing group at Chalmers University of Technology for their patient guidance, valuable advices and providing the opportunity to take part in the Strategic Research Centre on Microwave Antenna Systems (Charmant) and Chalmers Antenna Systems VINN Excellence Centre (Chase). What is more, I would like to thank Mr. Magnus Bonnedal, System Engineer in the Signal Processing group in RUAG Space, for his interest and effort to help me on the system design. His experience and advices benefit me a lot.

Second, thanks to my friends and all the people that contributed to this thesis and their time.

In the end, special thanks to Heng Yang, you make my life full of happiness. Thanks to my family, my brothers and sisters in law. Without their consistent support and encouragement, I could not achieve so much in my life and studies.

## Table of Contents

|   |     |
|---|-----|
| Abstract.....   | IV  |
| Acknowledgements .....  | III |
| 1 Introduction .....  | 1   |
| 1.1 Background .....  | 1   |
| 1.2 Purpose.....  | 1   |
| 1.3 Outline.....  | 2   |
| 1.4 Abbreviations and Acronyms .....                            | 2   |
| 2 Satellite System Design.....                                  | 4   |
| 2.1 Array Fed Reflector Antenna System .....                    | 4   |
| 2.2 Basic Concept for Beamforming Antenna Arrays.....           | 5   |
| 2.3 S Parameters .....  | 7   |
| 2.3.1 Properties of the S Matrix .....                          | 8   |
| 2.4 Beamforming Network.....                                    | 9   |
| 2.4.1 Beamforming Concept.....                                  | 9   |
| 2.4.2 Beam Sharing Technology .....                             | 9   |
| 2.4.3 Beamforming Algorithm for Array Fed Reflector System..... | 9   |
| 2.4.4 Linear Array Beamforming.....                             | 10  |
| 2.4.5 Beamforming Network Components: .....                     | 11  |
| 2.4.6 1 to 7 Power Splitter Formation .....                     | 15  |
| 2.5 Link Analysis .....   | 16  |
| 2.6 Frequency Reuse Scheme .....                                | 17  |
| 3 Onboard Receiver System Design .....                          | 19  |
| 3.1 Receiver System Description.....                            | 19  |
| 3.2 Receive Beamforming Network Analysis .....                  | 19  |
| 3.2.1 Antenna Array Geometry .....                              | 19  |
| 3.2.2 Receiver Beamforming Network Structure.....               | 21  |
| 3.2.3 Beamforming Network Scheme Comparison .....               | 22  |
| 3.3 Receiver System Noise .....                                 | 24  |
| 3.4 Receiver Carrier to Noise Ratio (C/N).....                  | 26  |
| 4 Simulation Results of the Receiver Network.....               | 27  |
| 4.1 Antenna Pattern at the Receiver Centre Frequency .....      | 27  |
| 4.2 Peak Gain Value for the 22 Beams.....                       | 28  |
| 4.3 Focal Beam Pattern.....                                     | 29  |
| 5 Onboard Transmitter Network Design .....                      | 30  |
| 5.1 Tx Beamforming Network .....                                | 30  |
| 5.2 Power Utilization Consideration.....                        | 31  |
| 5.2.1 Active Radiating Array .....                              | 32  |
| 5.2.2 Semi-Active Radiating Array.....                          | 32  |
| 5.3 Butler Matrix .....   | 34  |
| 5.3.1 Why 4*4 Butler Matrix? .....                              | 35  |

|   |    |
|---|----|
| 5.3.2 Ports Connection Rules for Beamforming Network and the BMPA ..... | 36 |
| 5.4 HPA Choice: TWTAs VS SSPAs .....                                    | 36 |
| 5.5 BMPA+ BFN or BFN+ BMPA.....   | 37 |
| 5.6 Disadvantages of the Butler Matrix Transponder .....                | 38 |
| 6 Simulation Results of the Transmitter System .....                    | 39 |
| 6.1 Peak Gain Value for the 22 beams .....                              | 40 |
| 6.2 Peak Power Value on Ground .....                                    | 41 |
| 6.3 Frequency Reuse Scheme .....  | 42 |
| 7 Onboard System Integration.....                                       | 44 |
| 7.1 S matrix for the Diplexer .....                                     | 44 |
| 7.2 Isolation Level between the Tx Ports and the Rx Ports.....          | 48 |
| 7.3 Cross Over between the Neighbouring Beams.....                      | 49 |
| 7.4 Error Vectors for the Transmitter Network .....                     | 52 |
| 7.4.1 Test Methodology .....  | 53 |
| 7.4.2 Simulation Results.....   | 53 |
| 7.5 Frequency Reuse (Side Lobe Level Measurement) .....                 | 67 |
| 7.5.1 Test Methodology .....  | 68 |
| 7.5.2 Simulation Results.....   | 68 |
| 8 Conclusions and Future Work .....                                     | 72 |
| References.....   | 73 |



# 1 Introduction

## 1.1 Background

For mobile communication via satellites, large reflector antennas (10-20m) are used. They are fed by an array of a few hundred radiators. The radiators are at L- or S-band and combine the receive and transmit function. A diplexer is used to separate receive from transmit. A transmit and a receive network connect the diplexer with the beam-forming computer or analog beamforming network via A/D and D/A converters. There are several possible topologies at the transmit side.

In order to form multiple beams simultaneously covering the entire Europe, multiple beam antennas (MBA) are used. Multiple beam antennas, which enjoy the benefits of flexible antenna pattern control if a beamforming computer is implemented and simultaneous multi-beam forming capabilities, achieve significant system performance improvement compared to mechanically steered antennas. Spatial filtering can be employed by multiple beam antennas with multi-beam pattern, which can enhance the performance of satellite mobile communication systems in terms of capacity, coverage and throughput. Thus, MBA will play an important role in future mobile satellite communication system establishment.

Beam forming network, which is used in satellite communications, is a key factor in a multi-beam antenna system, especially in array fed reflector antenna systems. Analog beamforming (ABF) method and digital beamforming (DBF) method are the two ways to realize phase and amplitude control in MBA. Although DBF provides a lot of advantages, such as beams can be assigned to individual users, easy to upgrade and optimize, microwave analog beamforming is quite popular as it is easier to implement with Microwave Monolithic Integrated Circuit (MMIC) technologies [1]. Thanks to this technique, microwave beamforming can miniaturize adaptive array antennas and gain expense advantages. What is more, microwave analog beamforming provides easy frequency and timing synchronization as the signal-to-interference-plus-noise ratio (SINR) increases due to combining the signal before the A/D converter [2]. Last but not least, the DBF suffers from high power consumption and high mass payload.

An MBA provides plenty of advantages: The cost of the multi-beam antenna is rather low compared to the conventional methods. In the conventional method, each beam is generated by a single antenna. The beams on the ground are then far apart and the gain at the beam edge is quite low. By employing MBA and feed sharing technology, we can generate multiple beams simultaneously and have a nice beam crossover level. In addition, the multi-beam system can be easily reconfigured by using a digital beam forming network. This increases the system flexibility and reliability.

## 1.2 Purpose

The purpose of this thesis is to model an array fed reflector antenna system for L or S band satellite communication. The work is implemented in Mathworks<sup>™</sup> Matlab and Simulink [3]. The principle for the array fed reflector antenna system is studied and the structure of the system is

modelled in Simulink.

The task is to model a realistic system containing the essential parts such as the onboard transmitter network and receiver network. An ideal structure needs to be built at the first step and a large and complex realistic system needs to be built piece by piece in the end.

An array fed reflector antenna consists of a lot of antenna elements which together constitute a quite complex system. Different parts about this complex system, such as the onboard power utilization, the intermodulation problems, the gain performance of each beam and the receiver noise calculation, should be considered, studied and simulated in an attempt to get a big picture about the whole system as well as the performance of this system. Simulink provides an intuitive way to model, simulate and analyze communication systems; it is a good tool to run system level simulation. Therefore, building a simple model in Simulink could be a good start.

### **1.3 Outline**

Chapter 1 gives a brief background of this thesis. Chapter 2 depicts the satellite system design problem and the necessary theoretical background which will be used in the following chapters. Chapter 3 illustrates the onboard receiver system design methodology and Chapter 4 shows the simulation result of the receiver system. Chapter 5 emphasizes on the onboard transmitter system design and Chapter 6 sketches the simulation results. Chapter 7 integrates the receive system and the transmit system by using duplexers. The system tolerance test results are also shown in this chapter. Finally, Chapter 8 discloses the results of this thesis work and the proposed future work.

### **1.4 Abbreviations and Acronyms**

|          |  |
|----------|--|
| Charmant | Strategic Research Centre on Microwave Antenna Systems |
| Chase    | Chalmers Antenna Systems VINN Excellence Centre        |
| AFR      | Array Fed Reflector                                    |
| MBA      | Multiple Beam Antenna                                  |
| DBF      | Digital Beam Forming                                   |
| ABF      | Analog Beam Forming                                    |
| BFN      | Beam Forming Network                                   |
| BMPA     | Butler Matrix power amplifier                          |
| GEO      | Geostationary  |
| HPA      | High Power Amplifier                                   |
| LNA      | Low Noise Amplifier                                    |
| Tx       | Transmitter  |
| Rx       | Receiver   |
| SSPA     | Solid State Power Amplifier                            |

TWTA

Travelling Wave Tube Amplifier

## **2 Satellite System Design**

### **2.1 Array Fed Reflector Antenna System**

This on board satellite communication system consists of the array fed reflector antennas, diplexers, high power amplifiers (HPAs), beamforming network (BFN), mixers, digital to analog (D/A) and analog to digital converters (A/D), and digital signal processing module. The transmit band is 2160-2200 MHz and the receive band is 1980-2025 MHz, respectively.

A distributed antenna array and a reflector are included in an antenna array reflector system. The formation of the beams of such a system is due to placing the antenna elements into different positions with respect to the focal point of the large reflector. L or S-band mobile satellite communications using GEO satellite is being developed to facilitate use of satellite mobile phones. A large deployable reflector, a feed system and a beam forming network are the essential parts in order to generate multiple beams, achieve frequency reuse and high gain performance. In our system, a 12 meter main diameter reflector antenna with 6.3 meter focal length is employed. The feed array consists of 42 antenna elements which could form 22 beams simultaneously by using beam sharing techniques. In fact, each beam is formed by 7 antenna elements with a hexagonal distribution and the centre element's amplitude is 10 dB higher than the lateral elements, which means a 10 dB tapering in order to increase the aperture size, fully use the reflector and achieve the best performance.

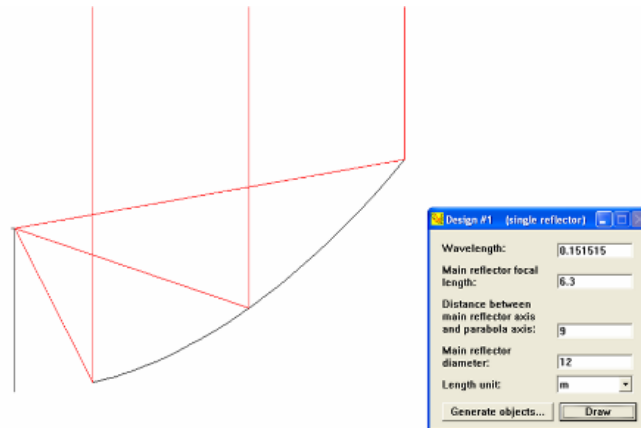


**Figure 2- 1 Reflector configuration**

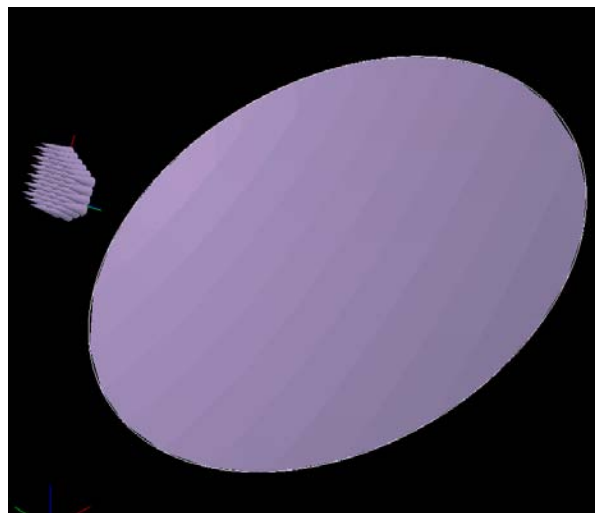


**Figure 2- 2 Array fed reflector**

## **2.2 Basic Concept for Beamforming Antenna Arrays**

### **Radiation Pattern**

Radiation Pattern refers to the relative radiation power distribution of an antenna as a function of the direction in space.

### **Main Lobe**

The main lobe of an antenna radiation pattern is the lobe containing the maximum radiation power.

### **Side Lobe**

Sidelobe means the lobes in any direction other than that of the main lobe in an antenna pattern.

### **Directivity**

Directivity is a figure of merit of antenna performance, which measures the fraction of maximum

radiation power compared to an isotropic radiator. It is defined as,

$$D(\varphi, \theta) = \max\left(\frac{4\pi \text{PowerRadiatedPerUnitSolidAngleInDirection}\varphi, \theta}{\text{TotalPowerRadiatedByAntenna}}\right) \quad (2.1)$$

### Antenna Efficiency

Antenna efficiency measures the ratio of the amount of power radiated into space by the total power received by the antenna.

### Antenna Gain

The maximum antenna gain is the product of the antenna efficiency and the antenna directivity. That is,

$$G = \eta D \quad (2.2)$$

### UV Coordinate

The UV coordinate is a common way to show the antenna radiation pattern using a transformation of the  $(\theta, \varphi)$  coordinates. Normally, we define  $U = \sin \theta \cos \varphi$  and  $V = \sin \theta \sin \varphi$ . Here,

$\theta, \varphi$  represent the azimuth and elevation angle of the three dimensional antenna pattern respectively.

### Effective Isotropically Radiated Power (EIRP)

The EIRP describes the product of transmitted power and antenna gain in terms of an equivalent isotropic source with power,  $P_t G_t$ , radiating uniformly in all directions.

$$EIRP = P_t G_t \quad (2.3)$$

### Effective Aperture

The effective area represents the amount of power that is captured from the passing plane wave and delivered to the antenna.

$$A_{eff} = \frac{\lambda^2}{4\pi} G \quad (2.4)$$

Normally, the radiation pattern of a single antenna element is quite wide with low directivity [4]. For satellite communication applications, because of the considerably large distance between the transmitter and the receiver, it is desirable to have very high gain antennas. For a GEO satellite communication system, the distance between the satellite and the earth is around 36,000 km. This will introduce a high free path loss which needs to be compensated by higher EIRP.

The constraint condition on wavelength and antenna size is  $\theta_{3dB}(\text{degrees}) \approx 70 * \lambda / d$  where  $\theta_{3dB}$  is the half power beamwidth,  $\lambda$  is the wavelength and  $d$  is the dimension across the antenna aperture. For a reflector antenna, the dimension  $d$  should be larger than  $10 * \lambda$ . Low frequency means that the wavelength is large, implying a large antenna, and vice versa. As the frequency increases the

antenna size reduces for a given beam width but the attenuation of the atmosphere increases. Thus there is a trade-off. Our system works in L or S band, where the atmosphere attenuation is rather small and can be neglected.

On the satellite side, normally a large reflector could be used to increase the beam gain. The gain of a beam is proportional to its 3 dB beam width and their relation is given by,

$$G \propto 1/(BW)^2$$

This relationship shows that the higher gain a beam has, the smaller will the beam width be. Smaller beam width means that more beams are needed in order to cover a certain area. The more beams we have, the more complex the system will be.

### 2.3 S Parameters

The S-parameters, which refer to the scattering matrix, is a useful method to quantify how RF power propagates through a multi-port network. The S-matrix allows us to represent a circuit or a complex network as a simple "black box". The external behaviour of this black box can be predicted and measured without knowing what is contained in it [5].

In an N port microwave network, power can propagate from any port (as input port) to any other ports (as output ports). The power can be reflected back as well. As both the magnitude and phase of the input signal could be changed by the network, S-parameters are complex containing the magnitude and phase information about the network. In general, these parameters are frequency dependent.

The S parameter matrix of an N-port network is a square matrix with  $N^2$  coefficients (S-parameters). They can be measured by sending a single frequency signal into the network or "black box" and detecting the signals exited from other ports. In the most basic sense, S-parameters refer to radio frequency (RF) "voltage out versus voltage in". If a wave is incident on one port, a part of the signal power is reflected back out of that port and other parts of the power exit from other ports. For the two ports network, the S-matrix has four S-parameters which are  $S_{11}$ ,  $S_{12}$ ,  $S_{21}$  and  $S_{22}$ . These four quantities are complex numbers with amplitude and phase information about the signal. Generally, we can write

$$\begin{bmatrix} V_1^- \\ V_2^- \end{bmatrix} = \begin{bmatrix} S_{11} & S_{12} \\ S_{21} & S_{22} \end{bmatrix} \begin{bmatrix} V_1^+ \\ V_2^+ \end{bmatrix} \quad (2.5)$$

or

$$[V^-] = [S][V^+] \quad (2.6)$$

where [S] is referred to as the scattering matrix. Examples of two ports and three ports S matrices are shown below.

$$\text{Two ports S-matrix: } \begin{bmatrix} S_{11} & S_{12} \\ S_{21} & S_{22} \end{bmatrix}$$

$$\text{Three ports S-matrix: } \begin{bmatrix} S_{11} & S_{12} & S_{13} \\ S_{21} & S_{22} & S_{23} \\ S_{31} & S_{32} & S_{33} \end{bmatrix}$$

By convention, we refer the “j” in the subscripts “ij” as the input port that is excited, and “i” as the output port. In this way,  $S_{ii}$ , refers to the signal reflected at Port “i” from the signal incident at the same port. It gives the ratio of the signal power incited and reflected on port ‘i’.  $S_{21}$  refers to the signal exited at Port 2 when the signal is incident at Port 1. The parameters along the diagonal of the S-matrix are referred to as reflection coefficients, while off-diagonal S-parameters are referred to as transmission coefficients [5].

For most devices, such as power dividers, amplifiers or attenuators, the magnitude is sometimes of the most interest. This is because the gain and loss of this network are more interesting to us in most cases. The magnitudes of S-parameters are presented in two ways, linear magnitude or decibels (dB). As S-parameters are voltage ratios, we have

$$S_{ij} (dB) = 10 \times \log_{10} |S_{ij}|^2 \quad (2.7)$$

because power is proportional to voltage squared.

### 2.3.1 Properties of the S Matrix

#### Unitary Property of the S matrix

For a lossless junction, the total input power equals to the total output power. Thus, the transpose of the S matrix is equal to the inverse of the complex conjugate of the S matrix. This is known as the unitary property of the S matrix [5]. This means that the sum of squares of the magnitudes of any row must equal unity. This does not hold for lossy N-ports. If any of the rows' sum-of-squares is less than one, there is a lossy element within the network, or something is radiating. The reason why we are using the sum of the squares instead of sum of the elements is because the S matrix is expressed in terms of voltage, and as we said before, we are accounting for power. Power is proportional to voltage squared.

#### Reciprocity

For an N by N network, which has N input ports and N output ports, some S-matrices are symmetric with respect to the leading diagonal. For the 2-port network, it means that  $S_{21} = S_{12}$ . This property guarantees that interchanges of the input and output ports do not influence the properties of the component. By using this property, power splitters and power combiners can be designed in the same way.

#### Frequency Dependency

S-parameters are defined for a given frequency and system impedance, and vary as a function of frequency for any non-ideal network [5].

To sum up, the S-parameters change with frequency, load impedance, source impedance and network. S-parameters are complex numbers which have both magnitude and phase information.

$S_{11}$  is the reflection coefficient and  $S_{21}$  describes the forward transmission coefficient. S matrix is a good way to describe electronic networks at high frequencies.

## **2.4 Beamforming Network**

### **2.4.1 Beamforming Concept**

Instead of using one antenna element, one could use more antenna elements (referred to as an antenna array) to increase the aperture area. The reason to do this is to shape the radiation pattern in a desired way with proper directivity. This can be achieved by feeding the same signal to different elements of an antenna array with appropriate amplitude and phase distribution. This process is known as beamforming [4]. By using beamforming, we can obtain the desired radiation patterns even for multiple beams at the same time.

One key issue in designing any beamforming network is to achieve desired amplitude and phase distribution at the N outputs of the RF network. In order to do so, power splitters/ combiners and phase shifters need to be included. Phase shifters can be implemented by inserting different lengths of the transmission lines between the power splitters and combiners for fixed beam pattern.

For a direct radiating array, the phase is mainly used to direct the beam, and the amplitude is used for sidelobe control. The simplest way to work with the beamforming is to only adjust the phase of signals from different elements to point the beam in a desired direction. This configuration offers low loss and good power efficiency, since the power amplifier could work with full load. But, the radiation patterns of this scheme are only limited by phase only beamforming, which could cause unacceptable side lobe levels. Another method to do the beamforming is using amplitude only optimization method, which provides poor power efficiency performance. Based on the limitations mentioned before, amplitude & phase optimization scheme is widely used. It shows poor power efficiency, but with very good radiation performance [6].

For an array fed reflector system, the feed array geometry is the mapping of the beam patterns on the ground. Thus exciting different antenna elements on the array will result in different coverage areas on the ground. The two FFT transforms from the feeds to the ground make the phase information not so interesting here.

### **2.4.2 Beam Sharing Technology**

The amplitude and phase applied to each array element is a complex quantity and throughout this work it is referred to as the excitation coefficient. If there is only one element, there is no way to change the pattern of an antenna even if the excitation changes. With two elements, however, changing the excitation coefficient of one element relative to the other will change the pattern. In order to generate multi-beams and shape the beam pattern, beam sharing technology is employed.

### **2.4.3 Beamforming Algorithm for Array Fed Reflector System**

In our application, we are using an array fed reflector antenna system. Figure 2-3 depicts the receiver beamforming algorithm for one beam. The task of the beamforming network is to control each sub array to cover a specific area on the ground. Thus for each beam, the output is calculated by [4]:

$$y(k) = \sum_{i=1}^7 w_i x_i(k) \quad (2.8)$$

In practical applications, the  $x_i(k)$  is normally a complex data with amplitude and phase information, and  $w_i$  is the weight which is controlled by the beamforming network.

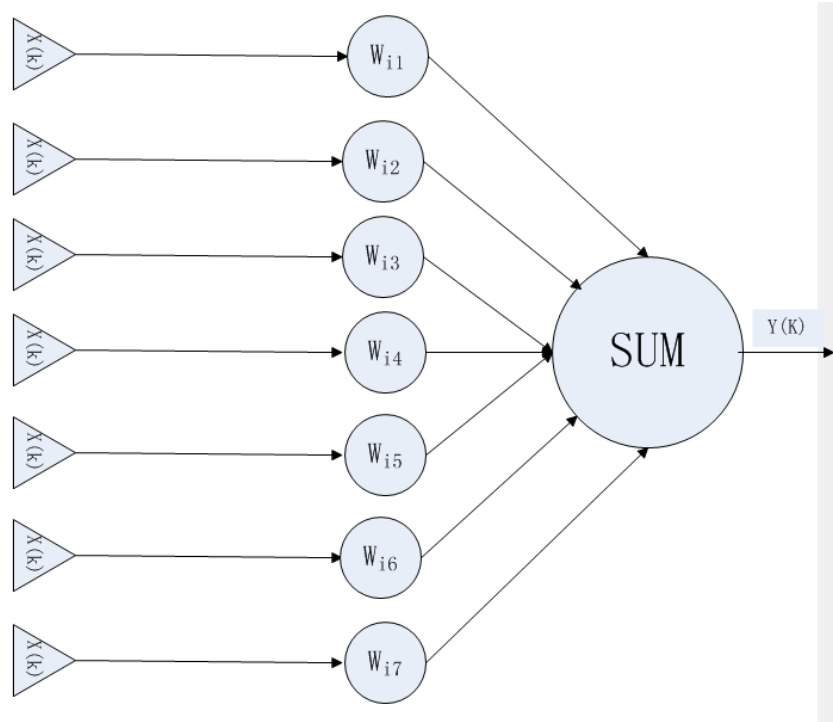


**Figure 2- 3 Beamforming architecture for the array fed reflector system**

#### 2.4.4 Linear Array Beamforming

Simulink provides an intuitive way to facilitate model based design. Figure 2-4 shows a simple linear planar array example which consists of 5 beam ports and 7 antenna elements to explain the beamforming algorithms. Each beam is formed by three antenna elements that are the centre element and its two neighbouring elements. The modulated signal from each beam port will be split into three parallel signals with desired amplitude and phase. Then these signals will be combined at the corresponding antenna input ports.

This example shows a MBA system which generates 5 beams on the ground. Neighbouring beams share one antenna element. Each beam covers a different geographical location with certain beam crossover level.

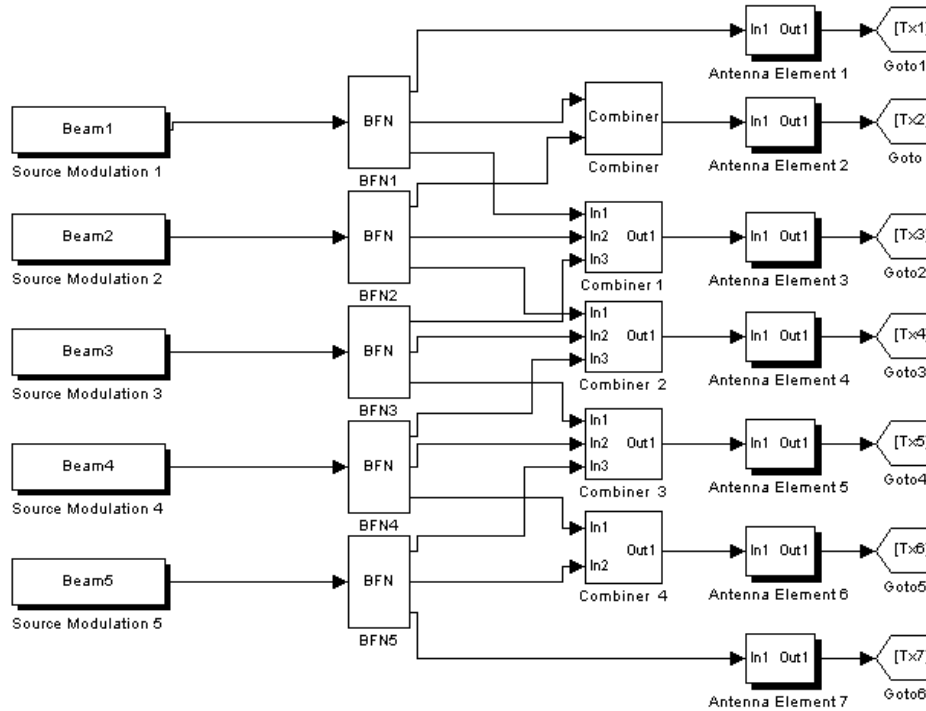


Figure 2- 4 MBA system in Simulink

## 2.4.5 Beamforming Network Components:

### Wilkinson Power Divider/Combiner

Power splitters/combiners are passive electronic components that are used for distributing or combining microwave signal power. A splitter can be used as either a power combiner or a power divider, it is a reciprocal device.

Ernest Wilkinson invented the Wilkinson power splitter around 1960. It could also be used as a power combiner due to the reciprocity. When working as a power splitter, it splits an input signal into two equal phase output signals, and it combines two equal-phase signals when it works as a combiner. It is a little bit tricky that a lossless reciprocal three-port network cannot have all ports simultaneously matched. In order to overcome this problem, Wilkinson added resistors in the network to allow all the ports to be matched. It can fully isolate the output ports at the centre frequency. An ideal Wilkinson splitter is 100% efficient. Here is a simple example of a three ports Wilkinson power splitter [7].

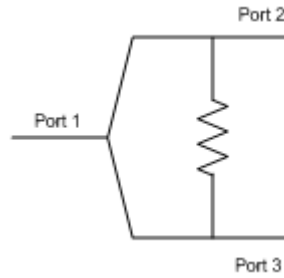


**Figure 2- 5 Three ports power divider**

The impedance at port 1 is different from that of ports 2 and 3. The impedances on arm 2 and 3 are larger than that of port one with a factor of square root of 2. When port 1 is excited, two signals with equal phase and amplitude will output from port 2 and 3. Because of the resistor, port 2 and port 3 are decoupled from each other. When it serves as a power combiner, the signal will be split equally between port 1 and the resistor R with none appearing at port 3 when port 2 is excited. Then port 2 and port 3 are well isolated. It is equally important to see that for a signal input at either port 2 or 3, half the power is delivered to port 1 and half is dissipated in the resistor.

Based on the work of Wilkinson, L. I. PARAD AND R, L. MOYNIHAN proposed a new kind of power divider, Split-Tee Power Divider [8]. This kind of power divider is a simple compact, broadband device when it is constructed in strip line. Similar to most of the power dividers in the microwave distribution network, it provides two isolated, equal phase, unequal amplitude output signals.

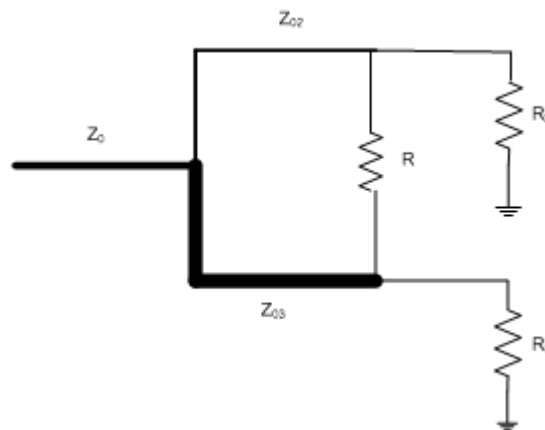


**Figure 2- 6 Power divider with unequal output impedance**

Consider the unequal power splitter as an example, which is shown in Figure 2-6. In such kind of power divider, when the power is fed into port 1, the output power at port 3 is  $K^2$  times that of port 2. Meanwhile, the voltage between the ground and arm 3 is equal to that between arm 2 and ground when measured at the same distance from port 1. How to achieve this? The answer is that the impedance on arm 2 needs to be  $K^2$  times the corresponding impedance on arm 3. Thus the characteristic impedances of the quarter-wave transformers in arms 2 and 3 can be determined as:

$$Z_{02} = Z_0 \sqrt{K(1 + K^2)} \quad (2.9)$$

$$Z_{03} = Z_0 \sqrt{\left(\frac{1+K^2}{K^3}\right)} \quad (2.10)$$

$Z_0$ ,  $Z_{02}$  and  $Z_{03}$  are the input impedance, impedance on arm 2 and impedance on arm 3, respectively.  $K^2$  is the power ratio between port 3 and port 2. By using these formulas, the voltages on arm 2 and arm 3 are equal at any distance from port 1. Hence, a resistor can be placed between these two arms without causing any power loss if the power is fed from port 1. However, when the power is fed from port 2 or port 3, part of the power will dissipate in the resistor. Another important function of this resistor is to achieve perfect isolation between port 2 and port 3. That means when the power is fed into port 2, part of the power will go to port 1, part of the power will dissipate in the resistor without any power leakage to port 3. The proper value for the resistor has not been derived yet, but normally we can choose  $R$  according to Equation (2.11). This yields an infinite isolation and a perfect match at the centre frequency.

$$R = Z_0 \frac{1+K^2}{K} \quad (2.11)$$

From Figure 2-6 and the discussion above, we can see that this network has unequal impedance levels, which results in that the scattering matrix is not that convenient to use in this case. Instead, another kind of scattering matrix, the un-normalized voltage scattering matrix is used to describe such a network. It is defined by:

$$\begin{bmatrix} d_1 \\ d_2 \\ d_3 \end{bmatrix} = \begin{bmatrix} T_{11} & T_{12} & T_{13} \\ T_{21} & T_{22} & T_{23} \\ T_{31} & T_{32} & T_{33} \end{bmatrix} \begin{bmatrix} c_1 \\ c_2 \\ c_3 \end{bmatrix} \quad (2.12)$$

Where  $d_i$  stands for the complex voltage wave (including amplitude and phase) departed from the  $i$ th-port and  $c_i$  stands for the complex voltage wave (including amplitude and phase) inserted upon the  $i$ th-port. The transfer coefficient  $T_{ij}$  is calculated by the following equations [8].

$$T_{11} = \Gamma \left[ 1 + \frac{(1-\Gamma^2)\ell^{-j2\theta}}{1+\Gamma^2\ell^{-j2\theta}} \right] \quad (2.13)$$

$$T_{12} = \left[ 1 + \frac{(1-\Gamma)^2\ell^{-j\theta}}{1+\Gamma^2\ell^{-j2\theta}} \right] \quad (2.14)$$

$$T_{12} = \frac{T_{21}}{K} \quad (2.15)$$

$$T_{13} = KT_{31} \quad (2.16)$$

$$T_{33} = \frac{2K^2}{1+K^2} \left[ \frac{Z_{2e}}{Z_{2e} + KZ_0} + \frac{1}{K^2(1+KY_{02}Z_0)} \right] - 1 \quad (2.17)$$

$$T_{23} = \frac{2K^2}{1+K^2} \left[ \frac{Z_{2e}}{Z_{2e} + KZ_0} - \frac{1}{(1 + KY_{02}Z_0)} \right] \quad (2.18)$$

$$T_{22} = \frac{2}{1+K^2} \left[ \frac{Z_{2e}}{Z_{2e} + KZ_0} + \frac{K^2}{(1 + KY_{02}Z_0)} \right] - 1 \quad (2.19)$$

$$T_{32} = \frac{2}{1+K^2} \left[ \frac{Z_{2e}}{Z_{2e} + KZ_0} - \frac{1}{(1 + KY_{02}Z_0)} \right] \quad (2.20)$$

Here,  $\theta$  is the frequency dependency factor:  $\theta = 90$  degrees means that the centre frequency corresponds to one quarter wavelength.

$$Y_{02} = \frac{1}{KZ_0} + \frac{1}{jZ_0 \sqrt{K(1+K^2)} \tan \theta} \quad (2.21)$$

$$Z_{2e} = Z_{02} \frac{Z_0(1+K^2) + jZ_0 \tan \theta}{Z_{02} + jZ_0(1+K^2) \tan \theta} \quad (2.22)$$

Although this kind of unequal output impedances achieves good Voltage Standing Wave Ratio (VSWR), isolation and phase identity, equal output impedance is much more popular in the application. Thus by introducing transformers into the network, see Figure 2-7, we can obtain the normalized S matrix.

$$\begin{bmatrix} V_1^- \\ V_2^- \\ V_3^- \end{bmatrix} = \begin{bmatrix} T_{11} & T_{12} \sqrt{\frac{Z_2}{Z_0}} & T_{13} \sqrt{\frac{Z_3}{Z_0}} \\ T_{21} \sqrt{\frac{Z_0}{Z_2}} & T_{22} & T_{23} \sqrt{\frac{Z_3}{Z_2}} \\ T_{31} \sqrt{\frac{Z_0}{Z_3}} & T_{32} \sqrt{\frac{Z_2}{Z_3}} & T_{33} \end{bmatrix} \begin{bmatrix} V_1^+ \\ V_2^+ \\ V_3^+ \end{bmatrix} \quad (2.23)$$

Here,  $Z_0$  is the input impedance at the input port,  $Z_2$  and  $Z_3$ , which are defined in Equations 2.9 and 2.10, are the load impedances at the output arms.

From the formulas provided above, we can see that the power divider is frequency dependent.

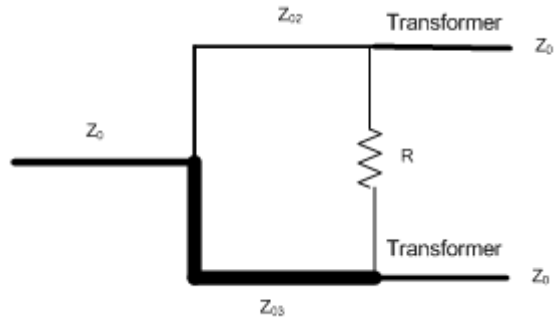


**Figure 2- 7 Power divider with impedance transformer**

**Phase Shifter**

This component is used to change the phase of the transmission coefficient. An ideal phase shifter introduces negligible loss of the transmit power. For simplification, we assume that the phase shifters are implemented by adding extra lengths of transmission lines in our beamforming network if necessary.

**2.4.6 1 to 7 Power Splitter Formation**

In the upper part, we only considered how to implement the 3 ports unequal power splitters. How can we apply this result to the 1 to 7 equal or unequal power splitters? The N-way Wilkinson unequal power splitter provides a solution to this problem [7]. However, we are using S matrix combining techniques to obtain the 1 to 7 equal or unequal power splitters in the software simulation. The process for designing equal power splitter/combiner and unequal power splitter/combiner is shown in Figure 2-8 and Figure 2-9. (Note: the line length and width are not proportional to its impedance).

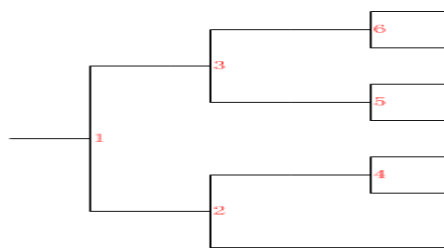


**Figure 2- 8 1 to 7 Equal Power Splitter/Combiner consisting of six unequal 1 to 2 splitters/combiners.**

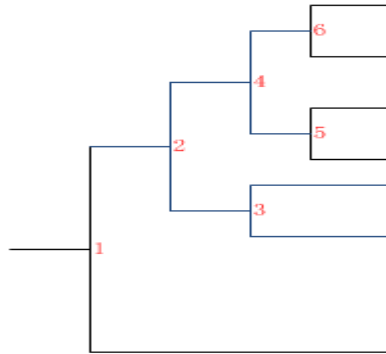


**Figure 2- 9 1 to 7 Unequal Power Splitter/Combiner consisting of six unequal 1 to 2 splitters/combiners.**

From these figures, we can see that the one to seven power splitter is formed by six one to two power splitters. First, we combine the S matrix for splitter 1 and 2 together. In the next step, we combine the resulting S matrix from step 1 with that of splitter 3. By doing so to the splitter 4, 5 and 6, we could obtain the S matrix for the one to seven power splitters. From the process, we can envision that the most critical part is to determine the power distribution ratio on these six splitters in order to achieve 10 dB tapering<sup>2</sup> between the centre element amplitude and its surrounding six antenna elements.

## 2.5 Link Analysis

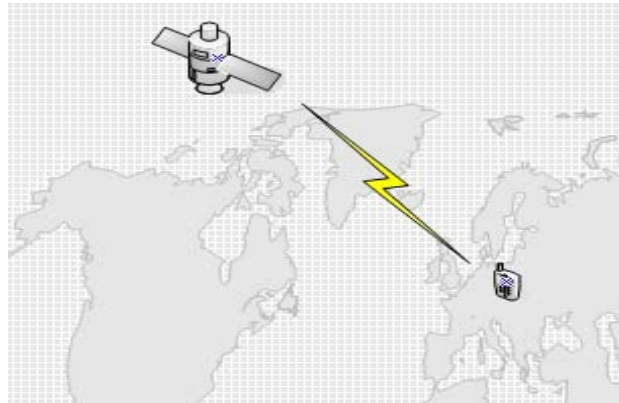


**Figure 2- 10 Satellite communication link**

The satellite communication links include uplink (from the earth to satellite), downlink (from satellite to earth) and inter-satellite communication links. In our system, the uplink and downlink performance is of great interest. By performing link analysis, we can identify the link quality such as the gains and losses of carrier to noise ratio and the hardware constraints.

### Free Path Loss

<sup>2</sup> This number is provided by RUAG Space. 10 dB tapering can give us a reasonable solution in terms of side lobe levels and reflector spill over.

As radio waves propagate in free space, the power decreases as a function of the distance squared. Due to the long path of a satellite communication link, the received power can be quite weak [9]. The free path loss can be expressed as:

$$L_{Fs} = \left( \frac{4 * \pi * R}{\lambda} \right)^2 \quad (2.24)$$

Where:

R is the distance from the receiver to the transmitter.

$\lambda$  is the wavelength of the transmitted radio signal.

The Friis transmission equation tells us that [9],

$$Pr = \left( \frac{Pt * Gt * Gr}{L_{Fs}} \right)^2 \quad (2.25)$$

$$EIRP = Pt * Gt \quad (2.26)$$

$$Pr(dBW) = EIRP(dBW) + Gr(dB) - L_{Fs}(dB) \quad (2.27)$$

Where,  $L_{Fs}$  means the free space path loss, Pr is the received power, Pt is the transmitted power, and Gt, Gr stands for the transmitter antenna gain and the receiver antenna gain, respectively.

It is assumed that the distance R is 36,000 km, the uplink frequency is 2GHz, the transmit power on the ground is 0dBW. The gain of the transmitter antenna is 3dBi and the beam gain of the satellite is 37dBi. The free pass loss is -189.6 dB and other losses are 3 dB. Thus, the received power at the satellite is -122.6 dBm (-152.6 dBW).

### **Carrier to Noise Ratio**

Carrier to noise ratio, usually expressed by C/N, is a useful characterization of the receiver system performance. High C/N ratios give better system performance, for example low bit error rate (BER). The noise analysis will be described in detail in Chapter 3.3.

### **G/T**

G/T is another figure of merit of a satellite receiver. It establishes a relation between the gain to system noise temperature, which provides a useful measurement for the quality of a receiver system.

## **2.6 Frequency Reuse Scheme**

In order to improve the system isolation performance and achieve a good frequency reuse, we go to the seven frequency reuse scheme. Figure 2-11 shows an example of the frequency distribution in this antenna array. It shows that beams 1, 14 and 16 are using the same frequencies which are all marked with a capital A. The subscripts stand for the beam number.

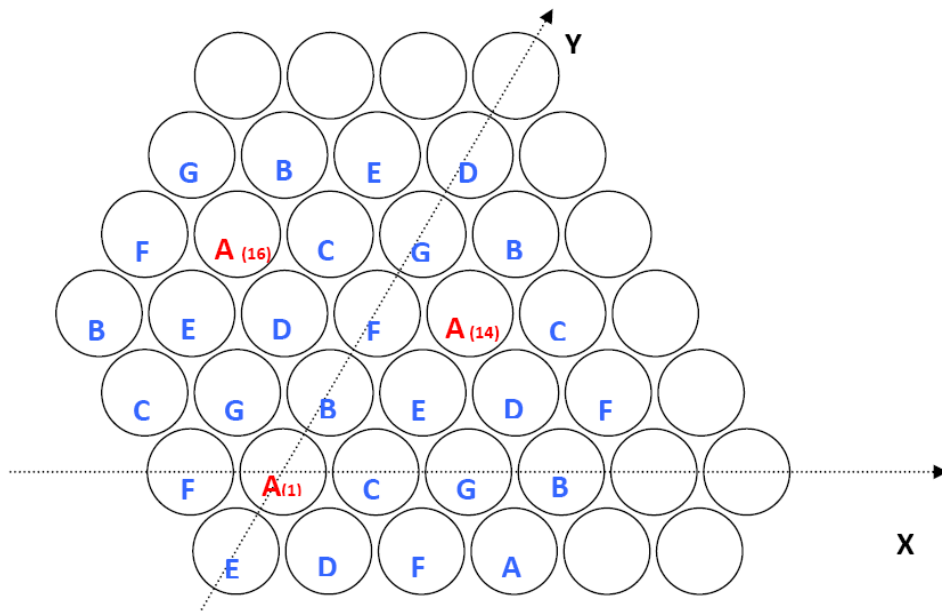


Figure 2- 11 Frequency reuse map

# 3 Onboard Receiver System Design

## 3.1 Receiver System Description

The receiver system is referred to as the receiver system on the satellite. As we can see from Figure 3-1, when the antenna array receives a signal from the earth, the signal will pass through the receiving antenna, the diplexer, and the low noise amplifier (LNA). The LNA is the most critical component of the receiver system. Low noise performance is of great interest. Besides that, the LNA also need to exhibit good gain and phase linearity and good voltage standing wave ratios (VSWR) over a broad bandwidth.

After the LNA, the signal reaches the beamforming network. It will be routed to the corresponding beam port without any leakage to other beam ports if the BFN is perfectly matched and isolated. After the BFN, a mixer will convert the RF signal to baseband. Then the signal will be demodulated, de-multiplexed and decoded. Remember that the reflector is located in front of the antenna array.

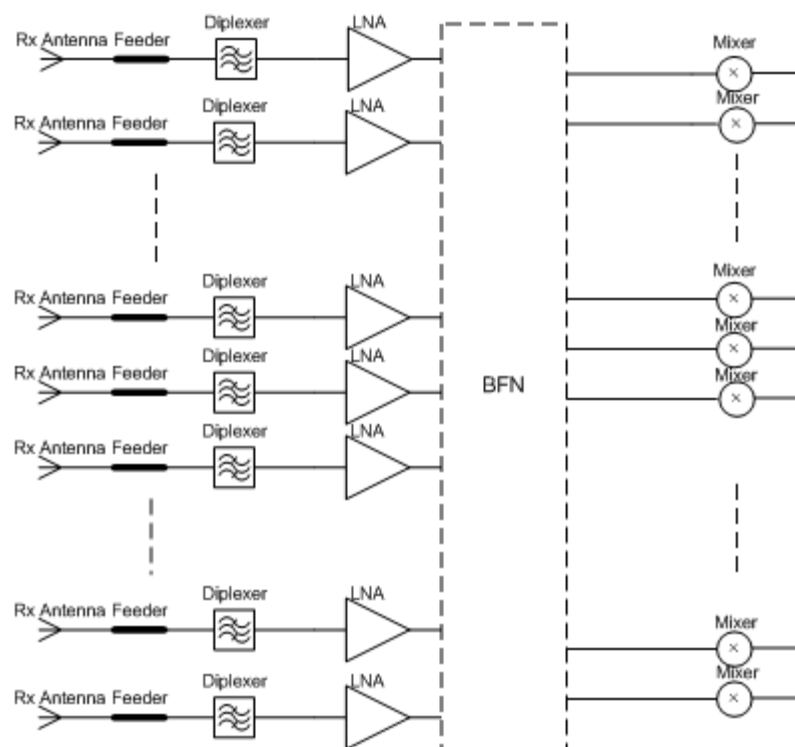
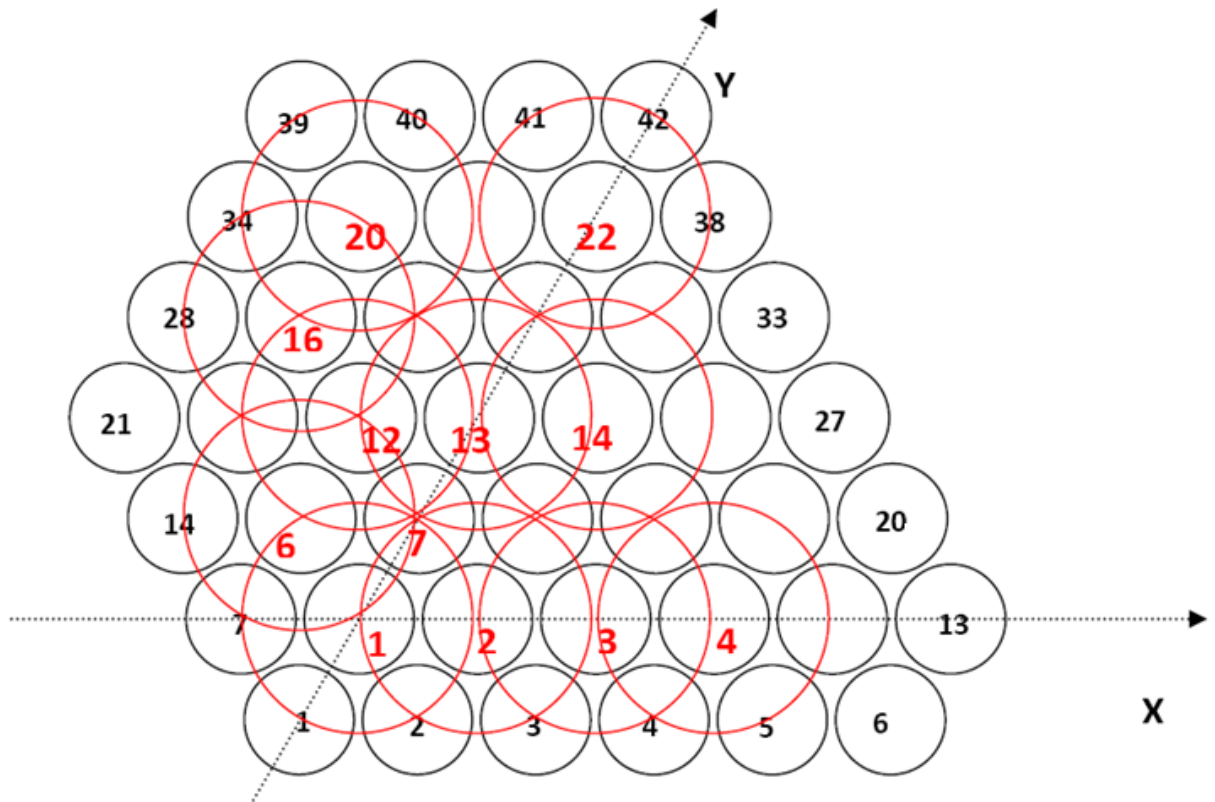


Figure 3- 1 Receiver system blocks

## 3.2 Receive Beamforming Network Analysis

### 3.2.1 Antenna Array Geometry

Figure 3-2 shows a picture of our antenna array geometry.



**Figure 3- 2 Antenna array geometry**

In our application, the antenna array has 42 antenna elements and intends to form 22 beams simultaneously in order to cover the whole of Europe. Feed sharing technique, which overcomes the dilemma between good beam-to-beam crossover level and reasonable aperture efficiency, provides a smart solution for satellite mobile communication. In order to use this method, a beamforming network (BFN) is needed. Seven feeds cluster and nineteen feeds clusters are widely employed in practice. In this paper, we are going to describe 7 feeds clusters in great detail. It could be easily extended to 19 feeds cluster and even more feeds.

Each beam is produced by 7 antenna elements and two adjacent beams share four feeds in our application. From Figure 3-2, we can see that the feeds are numbered from 1 to 42 and the beams are numbered from 1 to 22. Each beam is formed by one centre element and its six surrounding elements. The outer elements are only used for supporting the inner elements to form certain beams. For example, beam # 2 is formed by the antenna elements # 2, 3, 8, 9, 10, 16, 17. At the same time, beam # 8 is formed by the antenna elements # 9, 10, 16, 17, 18, 24, 25. They share the antenna elements # 9, 10, 16, 17.

Table 3-1 shows the beam numbering and antenna numbering method. The first column shows the beam number and the rest of the columns are the corresponding antenna elements number. For example, the first row means that antenna elements 1, 2, 7, 8, 9, 15 and 16 are used to form beam number 1 and the antenna element 8 is the centre element.

**Table 3- 1 Beam & Antenna Numbering Table**

| Beam Numbering | Corresponding Antenna elements |    |    |    |    |    |    |
|----------------|--------------------------------|----|----|----|----|----|----|
| 1              | 1                              | 2  | 7  | 8  | 9  | 15 | 16 |
| 2              | 2                              | 3  | 8  | 9  | 10 | 16 | 17 |
| 3              | 3                              | 4  | 9  | 10 | 11 | 17 | 18 |
| 4              | 4                              | 5  | 10 | 11 | 12 | 18 | 19 |
| 5              | 5                              | 6  | 11 | 12 | 13 | 19 | 20 |
| 6              | 7                              | 8  | 14 | 15 | 16 | 22 | 23 |
| 7              | 8                              | 9  | 15 | 16 | 17 | 23 | 24 |
| 8              | 9                              | 10 | 16 | 17 | 18 | 24 | 25 |
| 9              | 10                             | 11 | 17 | 18 | 19 | 25 | 26 |
| 10             | 11                             | 12 | 18 | 19 | 20 | 26 | 27 |
| 11             | 14                             | 15 | 21 | 22 | 23 | 28 | 29 |
| 12             | 15                             | 16 | 22 | 23 | 24 | 29 | 30 |
| 13             | 16                             | 17 | 23 | 24 | 25 | 30 | 31 |
| 14             | 17                             | 18 | 24 | 25 | 26 | 31 | 32 |
| 15             | 18                             | 19 | 25 | 26 | 27 | 32 | 33 |
| 16             | 22                             | 23 | 28 | 29 | 30 | 34 | 35 |
| 17             | 23                             | 24 | 29 | 30 | 31 | 35 | 36 |
| 18             | 24                             | 25 | 30 | 31 | 32 | 36 | 37 |
| 19             | 25                             | 26 | 31 | 32 | 33 | 37 | 38 |
| 20             | 29                             | 30 | 34 | 35 | 36 | 39 | 40 |
| 21             | 30                             | 31 | 35 | 36 | 37 | 40 | 41 |
| 22             | 31                             | 32 | 36 | 37 | 38 | 41 | 42 |

### 3.2.2 Receiver Beamforming Network Structure

Figure 3-3 illustrates a graphic view of the concept of the beam forming network.

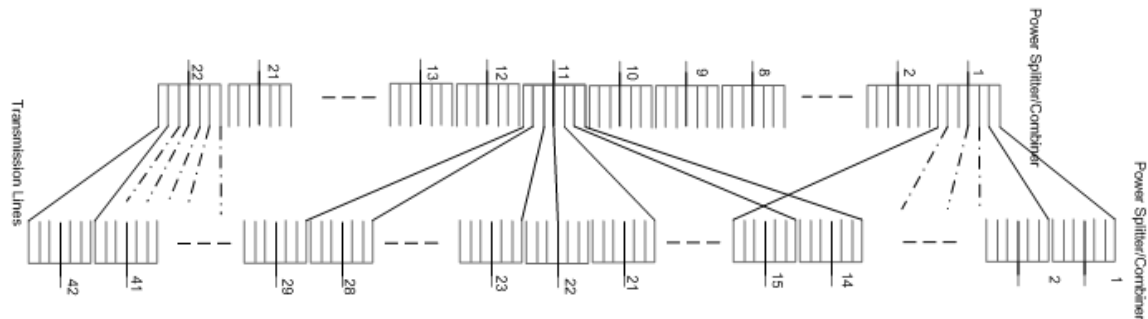


**Figure 3- 3 Beamforming network**

Basically, the BFN contains three parts: power splitter, power combiner and the phase shifters [10]. At the receiver side, the antenna elements receive signals from the ground. These signals will be

filtered and amplified before the BFN. At this stage, the received signal will be routed to the desired beam ports according to the beamforming algorithms.

### 10 dB Tapering

Sidelobe Level (SLL) is an important factor to measure the efficiency of the array radiation pattern. It is the amplitude of the highest sidelobe normalized to the main beam peak. When uniform excitation is used, it will generate sidelobes whose maximum amplitude is around -17dB in circular geometry in a direct radiating array. By using symmetric amplitude distribution with certain tapering, the SLL will be greatly reduced. In array fed reflector system, the tapering will influence the radiation pattern on the reflector. In fact, it is the reflector tapering that influences the sidelobe levels of our beams. We are using -10dB tapering. That means that the amplitude of the centre element in each cluster is 10 dB higher than the amplitude of its 6 surrounding elements. This is used to shape the antenna pattern and reduce the reflector spillover. Previous studies have shown that 10 dB tapering gives us a nice overall performance.

### 3.2.3 Beamforming Network Scheme Comparison

We proposed two schemes for beam forming network configuration. The first one is using unequal power combiners and equal power splitters. This configuration simplifies our port connection problem between the power combiners and power splitter. The second one is using unequal power splitters and combiners which are of the same type. The second scheme shows a better performance in terms of power loss. In addition, the using of the same component will simplify our design.

#### Case 1 Unequal Power Combiners + Equal Power Splitters

Consider beam 11 as an example.

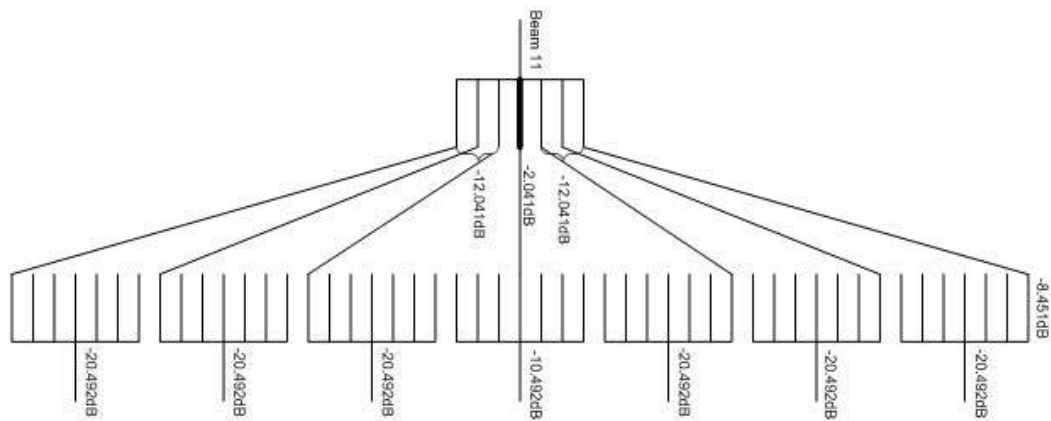


**Figure 3- 4 unequal power splitter and equal power combiner**

In order to achieve 10 dB excitation differences between the central element and its six lateral elements, we need to set the excitation coefficients difference between one branch and the other six branches of each unequal power combiner to be -10dB. The reason is that each equal power splitter introduces the same loss on its seven branches. Thus by controlling the coefficients on the power combiners, we can obtain the desired excitation coefficients distribution.

The simulation results show that the largest coefficient for each combiner is -2.041dB and the

remaining six are -12.041 dB. The excitation coefficient for the splitters is -8.451 dB ( $20 \cdot \log_{10}(1/\sqrt{7})$ ) for each branch. As a result, the total loss of the central element for this beamforming network is  $-2.041\text{dB} + -8.451\text{ dB} = -10.492\text{ dB}$ . The power loss on the 6 surrounding elements is  $-12.041\text{dB} + -8.451\text{ dB} = -20.492\text{ dB}$ .

### Case 2 Unequal Power Splitters + Unequal Power Combiners

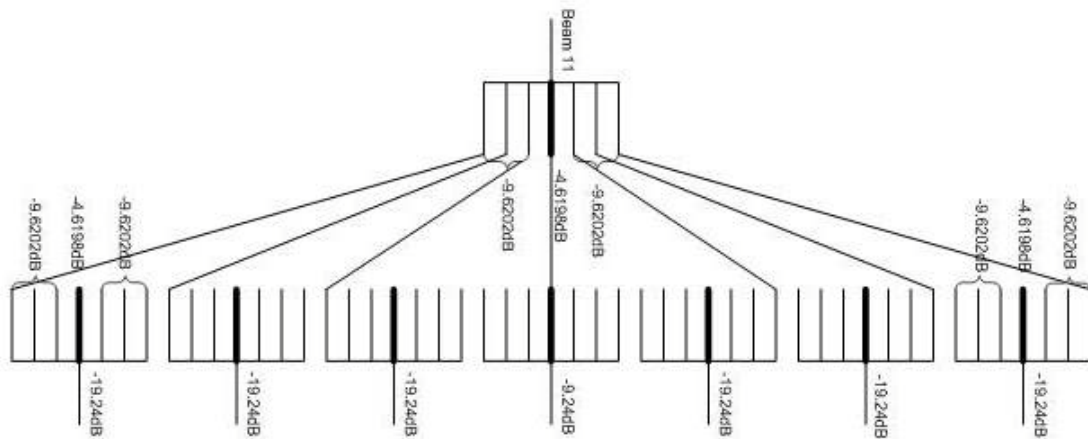


**Figure 3- 5 unequal power splitter + unequal power combiner**

In order to achieve 10 dB excitation differences between the central elements and the six lateral elements in this case, we need to set the excitation coefficients difference between the centre branch and the six remaining branches to be -5dB. This is because we are using unequal power combiner which introduces different losses between the central elements and the lateral elements. By connecting the largest coefficient in the splitter to the central element of the corresponding beam which has the largest coefficient in the combiner and connecting the smaller excited branches in the splitter to the smaller excited branches in the combiner, we can acquire the desired excitation coefficients in the antenna elements.

The simulation results show that the largest coefficient for each splitter is -4.6198dB and the remaining six coefficients are -9.6202 dB. The coefficients for the combiners are the same. As a result, the total loss of the central element for this beamforming network is  $-4.6198\text{dB} + -4.6198\text{dB} = -9.24\text{ dB}$ . The power loss on the six surrounding elements is  $-9.6202\text{ dB} + -9.6202\text{ dB} = -19.24\text{ dB}$ .

The advantage of the first case is that we can obtain the desired excitation coefficients by controlling the power distribution in the unequal power combiner. The splitters for all the antenna elements can be built in the same type. However, the second case introduces  $-19.24\text{ dB} - (-20.492\text{ dB}) = 1.252\text{ dB}$  less loss on each branch than the first case. Another advantage of the second case is we can use the same components for both splitters and combiners which are easy to manufacture.

### 3.3 Receiver System Noise

Figure 3-6 shows a simple graph view of the receiver system for one branch. The noise power associated with the link is specified by the system noise temperature  $T$ . Normally, it is made up from three contributions: antenna noise  $T_A$ , antenna - receiver connection, such as a cable or waveguide  $T_C$ , and receiver noise  $T_R$  which may include the RF, mixer and IF stage contributions [11]. The equation for the noise power calculation is:

$$N = KTB \quad (3.1)$$

Where  $k$  is Boltzmann's constant ( $k = 1.38 * 10^{-23} \text{ J/K}$ ) and  $B$  is the receiver bandwidth.

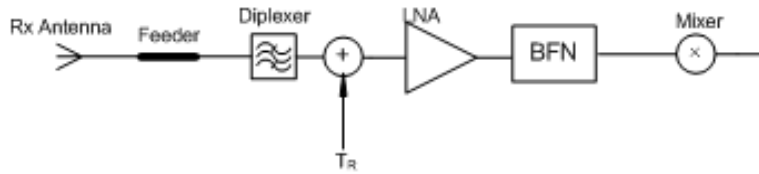


**Figure 3- 6 One branch of the receive system**

We can calculate the total receiver noise figure  $T_R$  from the individual contributions of cascaded circuits. The following Friis' noise calculation formula [11] can be used to calculate the receiver system noise:

$$T_R = T_{LNA} + \frac{T_{BFN}}{G_{LNA}} + \frac{T_{Mixer}}{G_{LNA} * G_{BFN}} \quad (3.2)$$

$$T_R = T_0 * (F_R - 1) \quad (3.3)$$

Here,  $F_R$  is the receiver noise figure and  $T_0$  is 290K (degrees Kelvin).

Equation (3.2) tells us that the noise temperature of the LNA and the gain of the LNA become the dominating factor to measure the system noise after the LNA stage. By placing this key component at the front-end receiver unit, the receiver noise figure is dominated by the first few stages. Because of the high gain and low noise properties of the LNA, the noise power of subsequent stages after the LNA is greatly reduced.

In our application, see Figure 3-6, we are interested in the system noise up to the beamforming network. Suppose the antenna temperature ( $T_A$ ) is 290K, the feeder network physical temperature ( $T_{fd}$ ) is 420K (130 °C) and its loss ( $L_{fd}$ ) is 0.1dB, the diplexer physical temperature ( $T_{dp}$ ) is 380K (90 °C) and its loss ( $L_{dp}$ ) is 0.3dB. (Note: These physical temperatures are provided by RUAG space. These are examples of the highest temperatures in the system during operation in space.) Figure 3-7 illustrates the receiver system specification for one path. These numbers are used to calculate the system noise in the worst case. For a two port case, the total output noise power  $T_{total} = T_s * \alpha + T_{phy} * (1 - \alpha)$ , where  $T_s$  is the noise source and the  $T_{phy}$  is the physical noise of the

network.  $\alpha$  is the loss coefficient [12].

$$Ts1 = Ta*(1/ Lfd) + Tfd *(1- 1/ Lfd) \quad (3.4)$$

$$Ts2 = Ts1*(1/ Ldp) + Tdp *(1- 1/ Ldp) \quad (3.5)$$

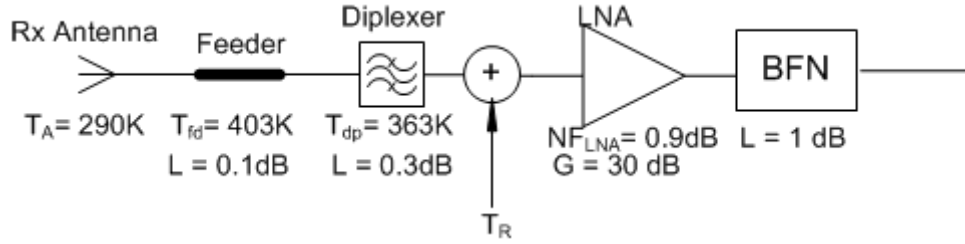


**Figure 3- 7 One branch of the receive system with specifications**

Equations (3.4) – (3.5) show the noise contribution at the receiver network consisting of two parts. The first part is the coherent noise which can be treated as a signal. The other part is the incoherent noise part which is generated by the components such as the feeder network, the diplexers, the LNAs and the BFN. In order to calculate the receiver system noise, we can treat these two parts separately. The gain of the LNA is not considered, because the LNA increases the system noise power and desired received signal power to a much higher level at the same time. At the receiver side, we are only interested in the signal to noise level.

We assume that all the beams only see the ground and the received antenna temperature will in this case equal to the ground temperature. We assume the ground temperature is 290 K, which is the input coherent noise to the onboard receiver system. It is shown as  $T_A$  in Figure 3-7. This noise can be treated as an input noise signal. It will be attenuated by the feeder network, the diplexer and routed to the corresponding beam port according to the beamforming algorithms. According to Figure 3-7, we can write the coherent noise as  $Ts2\_co = Ta / (Lfd*Ldp)$ . The output

noise voltage amplitude at the beam port is  $Ts\_co = \sqrt{Ts2\_co} * S$ .

The noise from the ground is coherent while the noise generated by the components in the receiver network is incoherent. The incoherent noise up to the input of the BFN can be expressed as  $Ts2\_inco = Tfd *(1- 1/ Lfd)/Ldp + Tdp *(1- 1/ Ldp) + (NF_{LNA} - 1) * 290$ . Consequently, the incoherent noise power at the beam port is calculated by  $Ts\_inco = Ts2\_inco * S * S^* = Nin * |S|^2$ , where  $S$  is the  $S$  matrix of the beamforming network and ‘\*’ means conjugate.

The noise power at the beam port consists of the incoherent noise power and the coherent noise power. Accordingly, the total noise power density at the beam port is  $N0 = ((Ts2\_co)^2 + Ts2\_inco) * k$ . The simulation results show that the noise power density is -204 dBW/Hz.

We need to mention that we assume the thermal radiation from every point on earth is coherent at all the antenna feeds. Hence we can treat the thermal noise received from earth as coherent signal. We use an approximation here in that we assume that the temperature is the same all over the earth, and do not have to take into account the actual beam coverage area.

### 3.4 Receiver Carrier to Noise Ratio (C/N)

From Chapter 3-3, we know the system temperature  $T_s$  (which includes antenna noise  $T_A$ , cable and receiver noise) [9]. Then the noise power (single link) at receiver input is:

$$N = KTB \quad (3.6)$$

Then, 
$$\frac{C}{N} = \frac{P_r}{N} = P_t * G_t * \left( \frac{G_r}{T_s} \right) * \frac{1}{L_{F_s}} * \frac{1}{k * B} \quad (3.7)$$

$$C/N(dBW) = EIRP(dBW) + Gr(dB) - L_{F_s}(dB) - (K * B * T_s)(dB) \quad (3.8)$$

Here,  $\frac{G_r}{T_s}$  is the figure of merit in the receiver side. The received power is calculated in Chapter 2.5, which is -152.6dBW. The receiver system noise power density is shown in Chapter 3.3, which is -204 dBW/Hz. In this manner, the carrier to noise power density is 51.4dBHz.

# 4 Simulation Results of the Receiver Network

## 4.1 Antenna Pattern at the Receiver Centre Frequency

The antenna pattern for all the antenna elements (42 elements) is shown in Figure 4-1. The simulation results show that the outer antenna patterns are worse than that of the centre ones. The working frequency is 2002.5 MHz which is the centre frequency of the receive band. Table 4-1 shows the maximum gain of each antenna element at this frequency.

**Table 4- 1 Peak gain for all the antenna elements**

|            |         |         |         |         |         |         |         |
|------------|---------|---------|---------|---------|---------|---------|---------|
| Antenna No | 1       | 2       | 3       | 4       | 5       | 6       | 7       |
| Peak Gain  | 41.566  | 42.8306 | 43.3198 | 43.0624 | 42.0971 | 40.4903 | 42.1204 |
| Antenna No | 8       | 9       | 10      | 11      | 12      | 13      | 14      |
| Peak Gain  | 43.7794 | 44.6308 | 44.7089 | 44.0628 | 42.7394 | 40.7815 | 41.9106 |
| Antenna No | 15      | 16      | 17      | 18      | 19      | 20      | 21      |
| Peak Gain  | 43.9569 | 45.1916 | 45.6446 | 45.3495 | 44.3361 | 42.6497 | 40.9084 |
| Antenna No | 22      | 23      | 24      | 25      | 26      | 27      | 28      |
| Peak Gain  | 43.3771 | 45.0209 | 45.8517 | 45.9091 | 45.2353 | 43.8867 | 41.9928 |
| Antenna No | 29      | 30      | 31      | 32      | 33      | 34      | 35      |
| Peak Gain  | 44.0456 | 45.2828 | 45.7356 | 45.4377 | 44.4184 | 42.2867 | 43.9544 |
| Antenna No | 36      | 37      | 38      | 39      | 40      | 41      | 42      |
| Peak Gain  | 44.8076 | 44.8821 | 44.2376 | 41.8255 | 43.1006 | 43.589  | 43.321  |

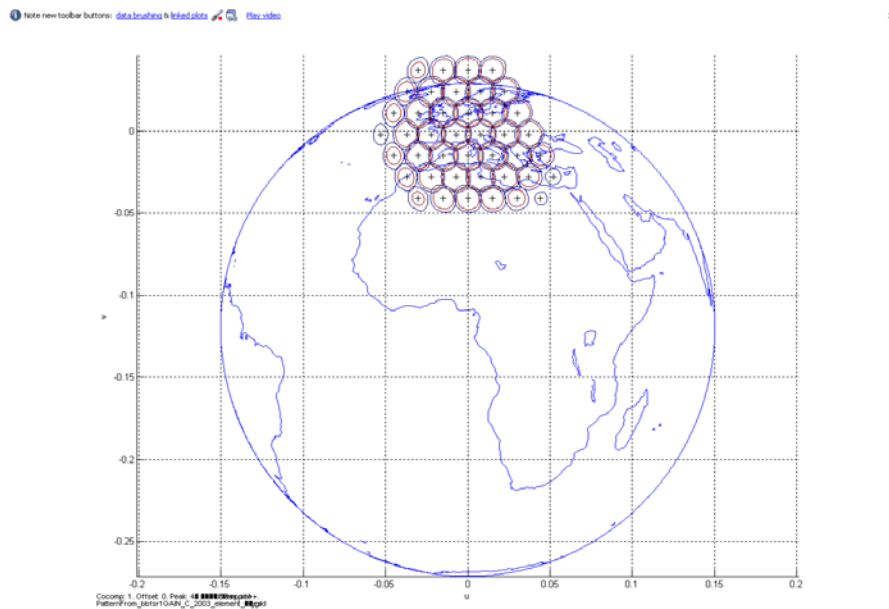


**Figure 4- 1 Antenna pattern for all the elements**

## 4.2 Peak Gain Value for the 22 Beams

As long as we know the antenna pattern for each antenna element in the receive band, we can use them to test the receiver network performance. The beamforming algorithm tells us that the radiation pattern of each beam is a sum of the radiation patterns of each 7 elements cluster. Table 4-2 shows the maximum gain for each beam by assuming the LNA gain is 30 dB and the filter loss is 0.3 dB.

**Table 4- 2 maximum gain of each beam**

|             |         |         |         |         |         |         |         |         |         |         |         |
|-------------|---------|---------|---------|---------|---------|---------|---------|---------|---------|---------|---------|
| Beam Number | 1       | 2       | 3       | 4       | 5       | 6       | 7       | 8       | 9       | 10      | 11      |
| Peak Value  | 66.6394 | 67.0667 | 67.1537 | 66.8959 | 66.3537 | 66.7047 | 67.3087 | 67.562  | 67.458  | 67.0404 | 66.429  |
| Beam Number | 12      | 13      | 14      | 15      | 16      | 17      | 18      | 19      | 20      | 21      | 22      |
| Peak Value  | 67.211  | 67.6407 | 67.7065 | 67.441  | 66.7476 | 67.3552 | 67.6102 | 67.5041 | 66.7108 | 67.1407 | 67.2272 |

From Table 4-1, we can see that the beam 14 has the largest peak gain among all the beams. We can also see that the edge beam peak power is a little bit less than the centre beams'. Centre beams like beam 7, 8, 9, 12, 13, 14, 17 and 18 have larger maximum gains compared to the outer beams such as beam 1, 2, 3, 4, 5, 6, 10, 11, 15, 16, 19, 20, 21 and 22. Figure 4-2 shows the beam patterns on the ground. The contour levels are 64 and 65 dB. Take beam 13 as an example, this beam is formed by antenna elements 16, 17, 23, 24, 25, 30 and 31. The antenna gains for these elements are shown in Table 4-1. Knowing the antenna gains, we can use them to calculate the beam gain according to the beamforming algorithms. We know that the LNA gain is 30 dB and the filter loss is 0.3 dB. After applying the beamforming algorithms, we obtain the peak gain for beam 13 as 67.6407dBi.

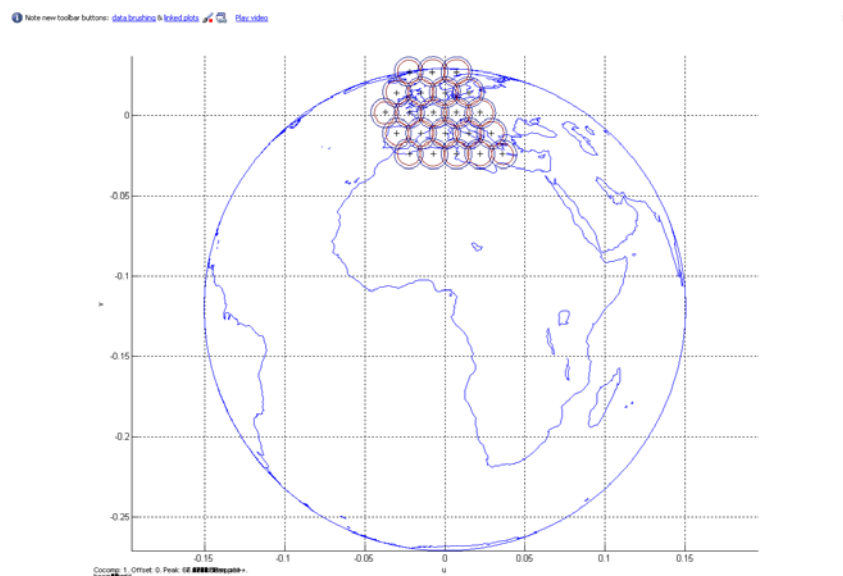


**Figure 4- 2 Beam pattern for all the beams**

### **4.3 Focal Beam Pattern**

Figure 4-3 shows the beam pattern for beam 13 which is the focal beam. It illustrates a nice beam pattern with maximum gain of 67.6 dBi and quite low side lobes.

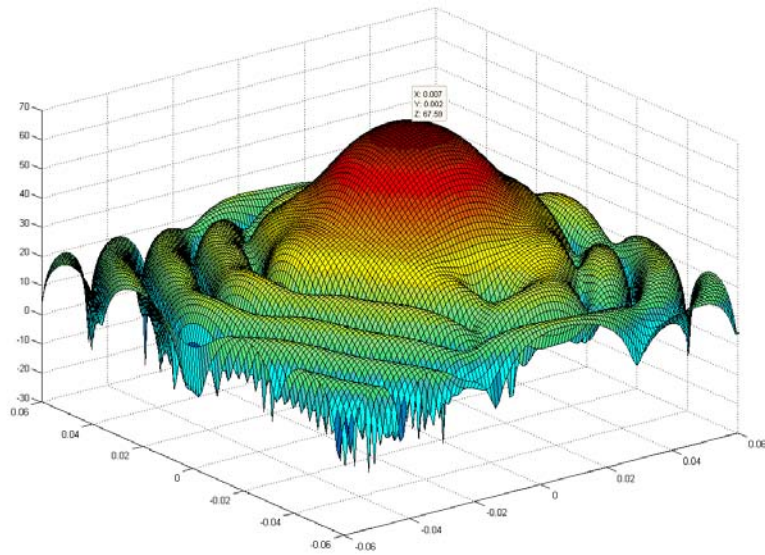


**Figure 4- 3 Beam pattern for Beam No.13**

# 5 Onboard Transmitter Network Design

The transmitter design is quite similar to that of the receiver. It mainly converts a baseband signal to RF signal with the LNA replaced by the high power amplifier (HPA). The most important factor we need to consider in the transmitter side is the efficient utilization of the onboard available power, especially when communicating with the satellite phones which are power and antenna gain limited devices. In such cases, high effective isotropic radiated power (EIRP) is needed in order to guarantee the link performance [13]. Figure 5-1 shows a picture of the transmitter system.

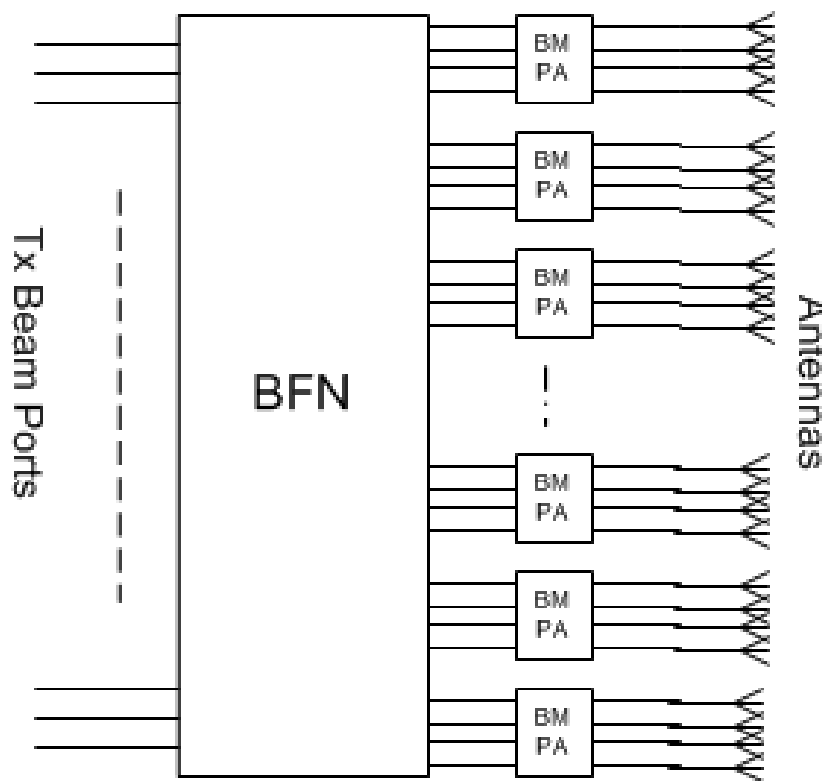


Figure 5- 1 Transmitter network

## 5.1 Tx Beamforming Network

The transmitter beamforming network structure is the same as the receivers'. It is shown in Figure 3-3 in Chapter 3. According to the figure, each one of the 22 power splitters split the power of one beam into its seven feeds according to the desired amplitude distribution, and the phase shifters distribute the signal with proper phase information. Then, every one of the 42 power combiners combines the power from its corresponding ports. The power splitter input ports are the beam ports and the power combiner output ports are the antenna elements ports.

By using the beamforming network, a single radiating antenna element can carry signals from different beams. Therefore, it results in beam overlap.

## 5.2 Power Utilization Consideration

Multiple antennas are used to shape the beam pattern with a higher directivity and much larger gain. Considering an active antenna array, according to the beamforming algorithms, each beam is formed by one centre element and its 6 surrounding elements. The outer antenna elements of the antenna array only perform supporting function, which means they need much less power compared to the inner antenna elements in the antenna array. The satellite is power limited and efficient utilization of the onboard power should be considered. For such reason, two types of amplifiers can be used to achieve this purpose if each antenna is driven by its own power amplifier. Figure 5-2 shows a distribution of the power load in all the antenna elements under such assumption. It shows that the inner antenna elements consume much more power than the outer antenna elements under the assumption that all the beams are fully loaded and the maximum antenna loading power is 100 Watt [14].

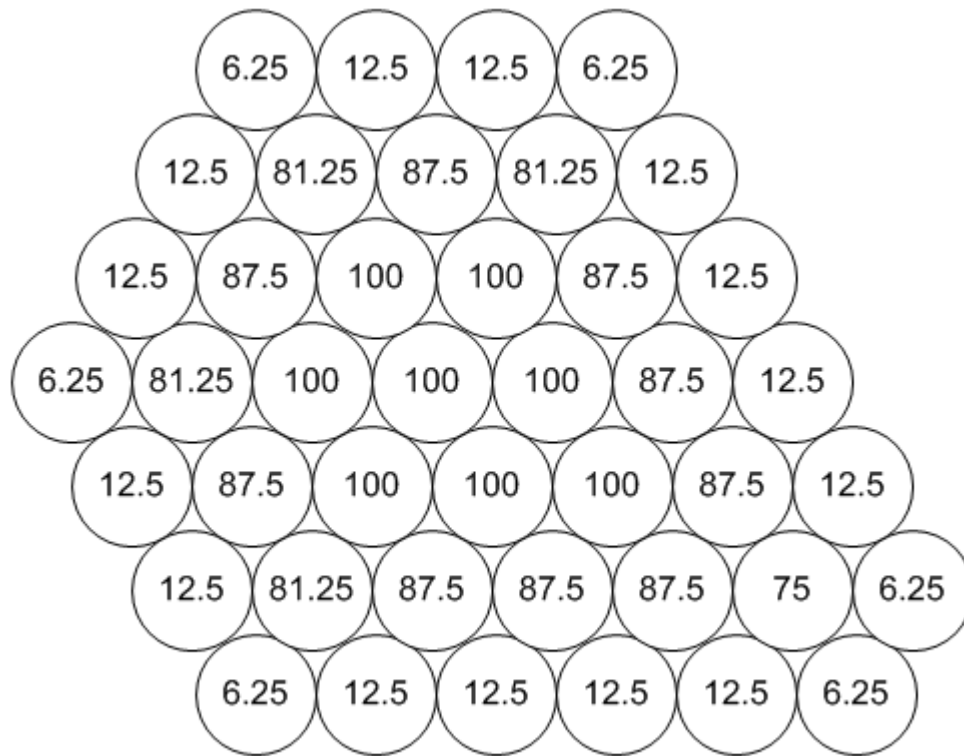


**Figure 5- 2 Power map for active radiating array**

In reality, the traffic distribution is unknown before the satellite is launched. It can vary with the time, geography position, population density and so on. This makes the power distributed non-uniformly since some beams will carry much more traffic than the others. The more traffic a beam carries the more power it needs to consume. It is quite desirable to move power from one beam to other beams for the purpose of efficient use of the onboard power. The utilization of the Butler matrices can efficiently solve this problem. The following sections will describe this in detail.

### **5.2.1 Active Radiating Array**

In order to achieve the maximum efficiency, the power amplifiers should operate as close to the saturation point as possible. In fact, the operating power level will influence the performance of the power amplifier. If the operating power level is too low, it is unable to achieve high power efficiency. If the power amplifier is overloaded, the nonlinearity would be a big problem to the system. In the active radiating array, the power is unevenly distributed in the antenna elements. This is because of the 10 dB power difference between the centre element and its six neighbouring elements. This phenomenon will cause the power amplifiers to become unevenly loaded which gives rise to the power inefficiency problem. This problem can be overcome by setting the operating point of each amplifier to produce an average output level substantially below the saturation output level. This guarantees a certain linearity, but results in very poor power efficiency. In addition, it will cause another problem if the power amplifiers are working in nonlinear stage. Adjacent beams share some antenna elements. If the seven amplifiers for the same beam have different power levels (this will result in different phase and amplitude performance of the amplifiers), the radiation pattern for such a beam will eventually be affected. This is because the different power level of the amplifiers will result in the phase and amplitude of the beamforming network to deviate from the desired distribution, which of course affects the antenna radiation pattern performance.

The traffic of each beam is unpredictable due to the reasons mentioned before. Thus it is difficult to make all the power amplifiers work in the most efficient way in the active radiating array.

### **5.2.2 Semi-Active Radiating Array**

The uneven power load for the active radiating array is unavoidable, because the power cannot move from one beam to other beams. But the power amplifiers should work as efficiently as possible on the satellite. In order to overcome this problem, a semi-active radiating array which consists of a beamforming network and a Butler matrix network after the antenna elements can be employed. The Butler matrix network works to even the power load for the power amplifiers in order to make them work as efficiently as possible. Some US patents proposed using Low Level Beam Forming (LLBF) and Hybrid Matrix Power Amplifier (HMPA) to achieve equal power amplifier loading [16]. Here we are going to use the Butler Matrix Power Amplifier (BMPA) to achieve this purpose. A 4 by 4 matrix is a good choice for our antenna geometry. The reason is explained in Chapter 5.3.1. Figure 5-3 shows our Butler matrix power amplifier (BMPA) design scheme. The first matrix is a typical Butler matrix and the second matrix is the image of the first one. Because of the evenly distributed load property of the Butler matrix, all power amplifiers will work with the same load behind the same Butler matrices. When entering either one port or a couple of ports of the first Butler input ports, the signal power will be divided into equal parts and amplified by all power amplifiers and ending up at the corresponding output ports of the second Butler matrix. The second Butler matrix routes the signal to the desired ports without power loss in ideal case. By doing so, the BMPA even the power load for the amplifiers and the signal transmission property will not be affected except for introducing the phase difference between the input signal and the output signal. Thus, the power amplifiers could work in the linear region and the intermodulation products can be greatly suppressed. What is more, there is no need to worry about losing a beam or carrier even if one of the power amplifiers fails. Another important

property of this system is that when bandpass filters are added after the BMPA stage, the carrier to intermodulation ratio can be greatly reduced if the intermodulation interference product is out of band.

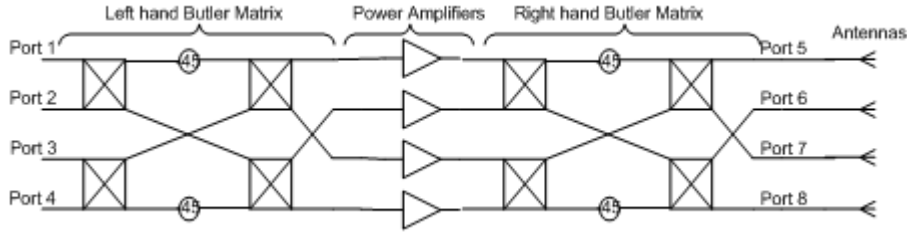


**Figure 5- 3 Butler Matrix Power Amplifier (BMPA)**

Equation 5.1 shows the S matrix for the BMPA in the ideal case, which means that the Butler matrix is lossless and the power amplifier nonlinear property is not considered. It is assumed that the power amplifier has a linear voltage gain. The transmission lines, which introduce phases, used to connect the couplers and hybrids of the Butler matrix are not included.

$$S_{BMPA} = \begin{bmatrix} 0 & 0 & 0 & 0 & 0 & 0 & 0 & 1\angle 225^\circ \\ 0 & 0 & 0 & 0 & 0 & 0 & 1\angle 225^\circ & 0 \\ 0 & 0 & 0 & 0 & 0 & 1\angle 225^\circ & 0 & 0 \\ 0 & 0 & 0 & 0 & 1\angle 225^\circ & 0 & 0 & 0 \\ 0 & 0 & 0 & 1\angle 225^\circ & 0 & 0 & 0 & 0 \\ 0 & 0 & 1\angle 225^\circ & 0 & 0 & 0 & 0 & 0 \\ 0 & 1\angle 225^\circ & 0 & 0 & 0 & 0 & 0 & 0 \\ 1\angle 225^\circ & 0 & 0 & 0 & 0 & 0 & 0 & 0 \end{bmatrix} \quad (5.1)$$

Equation (5.1) shows the property of the BMPA. When port 1 is excited, then the signal will end up at port 8 with a certain phase difference, -225 degree. But the power load at the power amplifier stage is the same for the four HPAs. In order to compensate the phase differences between the input and output signals, transmission lines can be added in length.

In this case, four antenna elements need to be grouped together and the grouping result is shown in Figure 5-4. The grouping method is depending on port connection rules which will be described later. The average power for each group is between 50W (17dBW) to 61W (17.8dBW) by assuming that all beams are at the maximum load. This is a great improvement compared to Figure 5-2. It can deal with coherent signals and power sharing technology is used to avoid uneven traffic load problem.

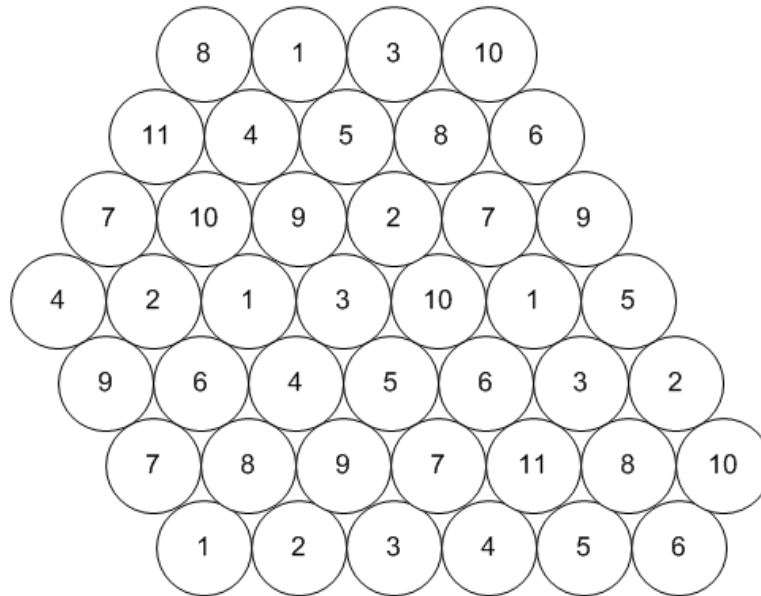


**Figure 5- 4 Grouping map**

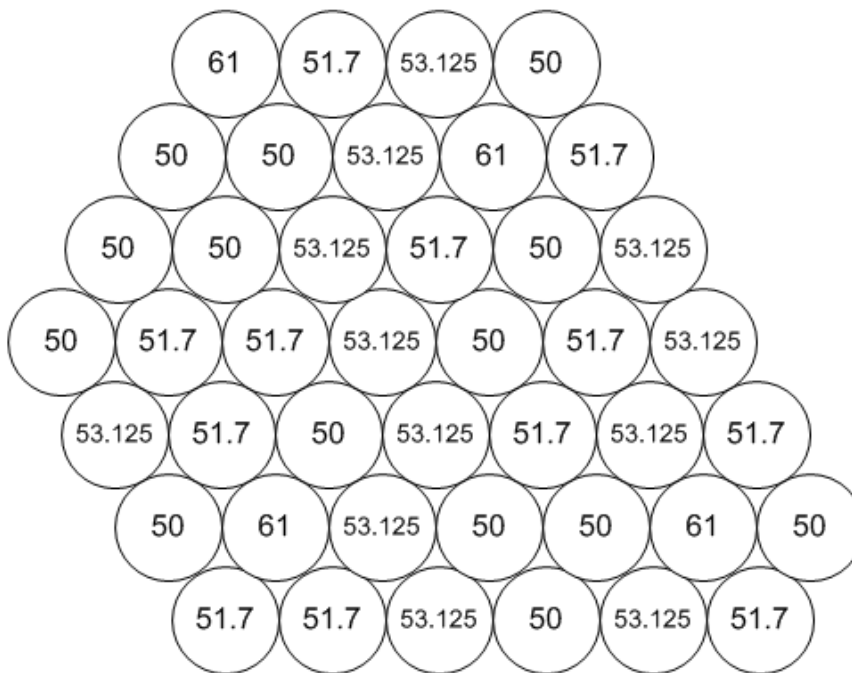


**Figure 5- 5 Power distribution map for semi-active radiating array**

### **5.3 Butler Matrix**

Normally, the Butler matrix is considered as a type of beamforming network using  $-90$  degree hybrids and  $-45$  degree phase shifters [15]. It has  $N$  input ports and  $N$  output ports, where  $N$  normally is 4, 8 or 16. Each Butler matrix network needs  $(N/2) * \log_2(N)$  hybrids and  $(N/2) * \log_2(N-1)$  phase shifters. The Butler matrix has two main functions: the first one is that it performs a Fast Fourier Transform (FFT) and can generate  $N$  orthogonal beams simultaneously; the second

property of the Butler matrix is that it is able to even the output power from different input ports. In our design, the beamforming network undertakes the beamforming function. Thus, the beamforming property of the Butler matrix is not of great interest. However, its second property can be used to greatly improve the power amplifiers efficiency as is shown in the previous section.

The topology of a 4\*4 Butler matrix is shown in Figure 5-6, and the corresponding phase shift characteristics are shown in Table 5-1.

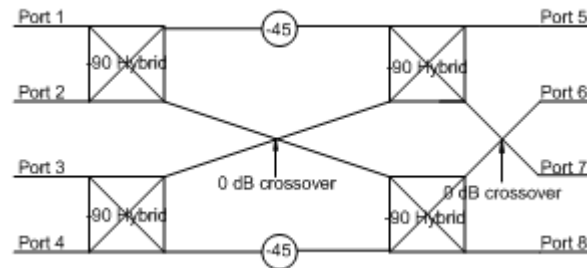


**Figure 5- 6 Butler matrix**

**Table 5- 1 Phase Distribution of the 8 Ports Butler Matrix**

| input ports /<br>output ports | Port 1 | Port 2 | Port 3 | Port 4 |
|-------------------------------|--------|--------|--------|--------|
| Port 5                        | -45    | -135   | -90    | -180   |
| Port 6                        | -90    | 0      | -225   | -135   |
| Port 7                        | -135   | -225   | 0      | -90    |
| Port 8                        | -180   | -90    | -135   | -45    |
| Phase<br>difference           | -45    | +135   | -135   | +45    |

### 5.3.1 Why 4\*4 Butler Matrix?

There are two unavoidable problems for a beamforming network combined with a hybrid power amplifier scheme. The first one is HMPA port selection in order to obtain uniform or nearly uniform power distribution among the amplifiers. The port selection is important because the Butler matrix power amplifier network should be able to handle coherent signals [16]. A large Butler matrix will complicate this problem. Another problem is that the HMPA accommodation and layout. A 4 by 4 Butler matrix consists of 4 hybrids and two 45 degree phase shifters, while an 8 by 8 Butler matrix includes 12 hybrids and more phase shifters. Compared to an 8 by 8 Butler matrix, the 4 by 4 Butler matrix is easy to manufacture and has less loss and is less sensitive to the hybrid inaccuracies. In practice, the more hybrids involved the more inaccurate the system will be. Those smaller Butler matrixes have lower insertion loss as well as total mass and size. If taking advantage of 4 by 4 Butler matrixes, 11 groups of Butler matrix are needed. This is larger than the number of elements to form one beam. This provides a high probability to achieve near uniform distribution of all the power amplifiers. Each Butler matrix group only needs to drive one element for each beam, which will greatly simplify the port selection.

On the other side, a 2 by 2 Butler matrixes can only provide a small degree of power sharing between different beams, so it is not of great interest.

### **5.3.2 Ports Connection Rules for Beamforming Network and the BMPA**

By properly selecting the connections between the output ports of the beamforming network and input ports of the left hand butler matrix, uniform or near uniform power loading among the power amplifiers can be obtained. The rules for this system is avoiding coherent signal input to the same 4 by 4 Butler matrix and even the power load of all beams. Consider Figure 5-6 as an example. If the same signal is input to port 1 and 3 or port 1 and 4, we will see different power levels at the four output ports. Uneven power load of the PA stage will show up and destroy our beamforming algorithm in the end. Thus the signal from the same beam needs to be input to different Butler matrices to avoid this problem in our case.

The beamforming network outputs several coherent signals to multipoint of the BMPA. If a large HMPA was used, then the port selection would be very difficult in order to process coherent input signals [16]. Thus, a smaller BMPA can be used to overcome this problem. A 4 by 4 BMPAs is a smart choice. Seven branches of the beamforming network output the same signal. It is quite easy to distribute these 7 branches to the eleven BMPA groups without the same signal input to the same BMPA. Based on this idea, we can group the antenna elements in such a way as shown in Figure 5-4. It shows that antenna elements 1, 23, 26, 40 are connected to BMPA 1, elements 2, 20, 22, 31 are connected to BMPA 2, and so on. Thus, the BMPA 1 evens the power from output ports 1, 23, 26, 40 of the beamforming network and the BMPA 2 evens the power from output ports 2, 20, 22, 31 of the beamforming network. The beamforming network output ports 1, 23, 26 and 40 carry power from beam 1, beam 6, beam 7, beam 11, beam 12, beam 13, beam 29, beam 30, beam 18, beam 19, beam 25, beam 26, beam 32, beam 35 and beam 36. These powers from different beams will be evened out at the BMPA stage. According to such grouping method, all the power amplifiers can work almost at the same power load which results in great power efficiency improvement. In addition, the intermodulation products can be routed to out of band by using some other advanced ports connection rules. The intermodulation interference can be greatly suppressed in this way.

### **5.4 HPA Choice: TWTAs VS SSPAs**

Both Travelling Wave Tube Amplifiers (TWTAs) and Solid State Power Amplifiers (SSPAs) are widely used in the space applications. The TWTAs were the only option for space system designers 50 years ago and they account for a large market share nowadays [17]. TWTAs are capable of generating higher output power and working in high temperature and power density environment. TWTAs have broadband property and can operate in a large range of power levels; even low noise property is available. Their efficiency increases with the power level and frequency compare to SSPAs which work better in lower power applications. But recently, the application of SSPAs is becoming popular due to several reasons. SSPA is suitable for low power applications. It is generally known that TWTAs are slightly more reliable than SSPAs. But due to the current technology, the difference on reliability is negligible. Thanks to the current technology, SSPAs have achieved great development. They could work in almost all the frequency band including Ku band (12 to 18 GHz) [17].

Power amplifier normally is a single direction device, which means it could only amplify signal in one direction. The existence of an open line or a short circuit after the HPA will reflect the high

power signal back to the HPA. It will be destroyed if the reflected power is not dealt properly. Thus a circulator and a matching load need to be added at the HPA stage to avoid this problem. If coming from the other direction, the power will be circulated to zero. This is an important way to protect the high power amplifiers if there is high power reflected back to the power amplifier.

## 5.5 BMPA+ BFN or BFN+ BMPA

Both schemes can flexibly deliver power to the antenna elements. The first scheme is a simple design and adjustment but it will increase the feed loss due to processing the signal at high power levels [18]. The second scheme will make the power amplifiers work in uniform or near uniform power level without introducing too much power loss. Thus the second scheme, as shown in Figure 5-8, is preferred.

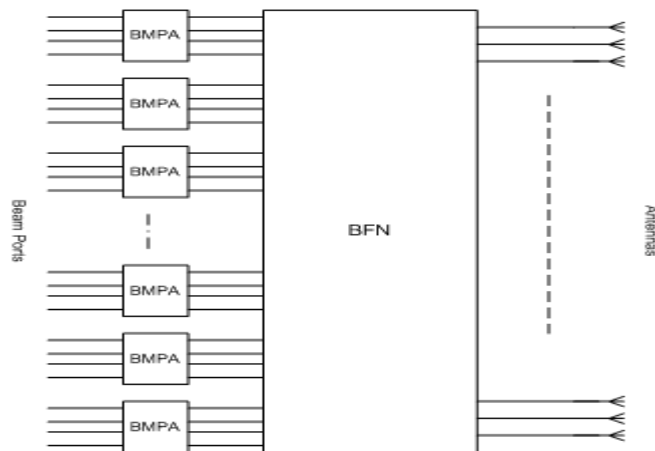
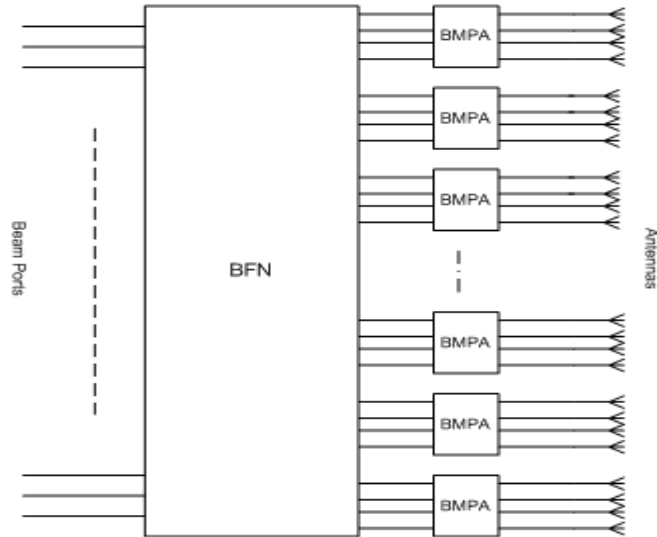


Figure 5- 7 Transmitter Network Structure 1



**Figure 5- 8 Transmitter Network Structure 2**

## **5.6 Disadvantages of the Butler Matrix Transponder**

The Butler matrix transponder has some drawbacks. Such kind of system needs multiple channel operation. With the increase of the number of beams and the number of feed elements to form each beam, the process to obtain a uniform or near uniform power distribution between the PAs becomes quite complex. What is more, the right hand butler matrix introduces power loss which is proportionally  $(N \cdot \log(N))$  to the order of hybrids. Nonetheless, compared to the advantages of using butler matrix, these disadvantages are a piece of cake.

# 6 Simulation Results of the Transmitter System

Table 6-1 depicts the maximum antenna gain for all the antenna elements in the transmit centre frequency, 2180 MHz. Figure 6-1 illustrates the contour plot for all the antenna elements and contour levels are 40 dB and 41 dB.

**Table 6- 1 Peak gain for all the antenna elements at 2180 MHz**

|            |         |         |         |         |         |         |         |
|------------|---------|---------|---------|---------|---------|---------|---------|
| Antenna No | 1       | 2       | 3       | 4       | 5       | 6       | 7       |
| Peak Gain  | 42.1134 | 43.5208 | 44.0491 | 43.7179 | 42.5738 | 40.7277 | 42.7347 |
| Antenna No | 8       | 9       | 10      | 11      | 12      | 13      | 14      |
| Peak Gain  | 44.5978 | 45.549  | 45.613  | 44.8451 | 43.2931 | 41.0401 | 42.5052 |
| Antenna No | 15      | 16      | 17      | 18      | 19      | 20      | 21      |
| Peak Gain  | 44.794  | 46.1875 | 46.6763 | 46.3174 | 45.13   | 43.1727 | 41.3972 |
| Antenna No | 22      | 23      | 24      | 25      | 26      | 27      | 28      |
| Peak Gain  | 44.1317 | 45.9792 | 46.9088 | 46.955  | 46.1531 | 44.5873 | 42.5686 |
| Antenna No | 29      | 30      | 31      | 32      | 33      | 34      | 35      |
| Peak Gain  | 44.8687 | 46.2627 | 46.7461 | 46.3882 | 45.2021 | 42.8733 | 44.7372 |
| Antenna No | 36      | 37      | 38      | 39      | 40      | 41      | 42      |
| Peak Gain  | 45.6898 | 45.7559 | 44.9802 | 42.3086 | 43.7194 | 44.2522 | 43.9263 |



shown in Table 3-1, this beam is formed by antenna elements 17, 18, 24, 25, 26, 31 and 32. The antenna gains for these elements are shown in Table 6-1. Knowing the antenna gains, we can use them to calculate the beam gain according to the beamforming algorithms. We know the HPA gain is 30dB. After applying the beamforming algorithms, we obtain the peak gain for beam 14 is 67.9dBi. The losses in the filters are not considered in this case.

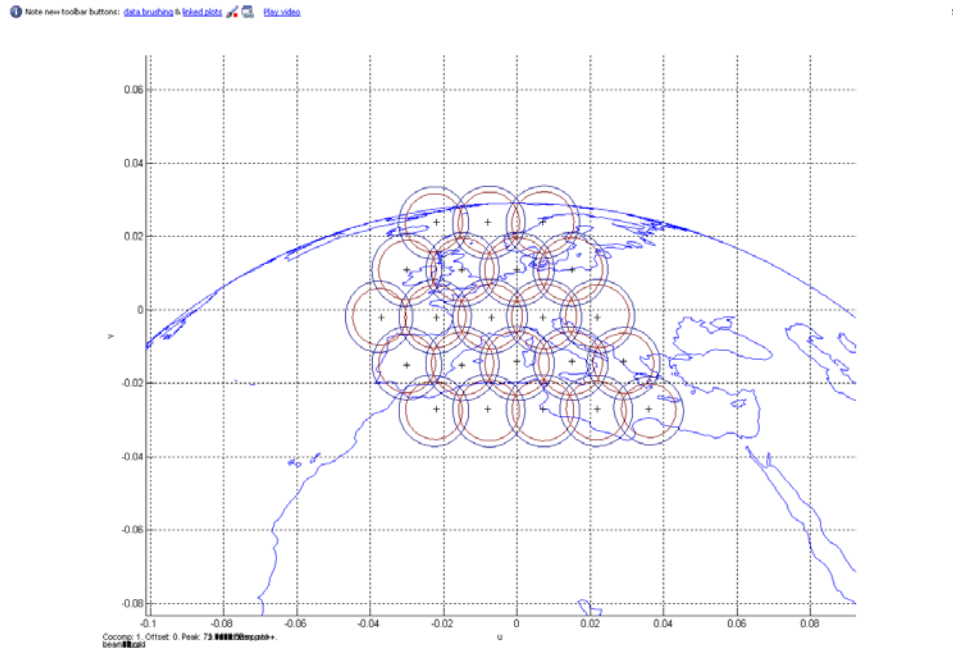


**Figure 6- 2 Beam pattern for the 22 beams**

## 6.2 Peak Power Value on Ground

The GEO satellite is located about 3,6000 km above the earth. Suppose the downlink frequency is 2.18GHz and the transmit power is 50 dBm. The maximum beam gain is shown in Table 6-2. Thus, the power received on the ground can be calculated. Figure 6-3 shows the power contour map for each beam on the ground. The contour levels are -76 dBm and -75 dBm. We know the free pass loss is -190.34 dB which is calculated according to the equations in Chapter 2.5. We assume other losses are 3 dB. Take beam 14 as an example. The transmit power is 50dBm and the beam gain is shown in Table 6-2. Thus the received peak power on the ground is  $50\text{dBm} + 67.93\text{dB} - 190.34\text{dB} - 3\text{dB} = -75.4 \text{ dBm}$ .

**Table 6- 3 Maximum gain of each beam on ground**

|             |          |          |          |          |          |          |          |          |          |          |          |
|-------------|----------|----------|----------|----------|----------|----------|----------|----------|----------|----------|----------|
| Beam Number | 1        | 2        | 3        | 4        | 5        | 6        | 7        | 8        | 9        | 10       | 11       |
| Peak Value  | -76.508  | -76.0673 | -75.982  | -76.2525 | -76.8289 | -76.4306 | -75.8093 | -75.5445 | -75.6545 | -76.1111 | -76.7208 |
| Beam Number | 12       | 13       | 14       | 15       | 16       | 17       | 18       | 19       | 20       | 21       | 22       |
| Peak Value  | -75.9215 | -75.4737 | -75.4077 | -75.6986 | -76.4013 | -75.7795 | -75.5149 | -75.6256 | -76.4485 | -76.0073 | -75.9288 |

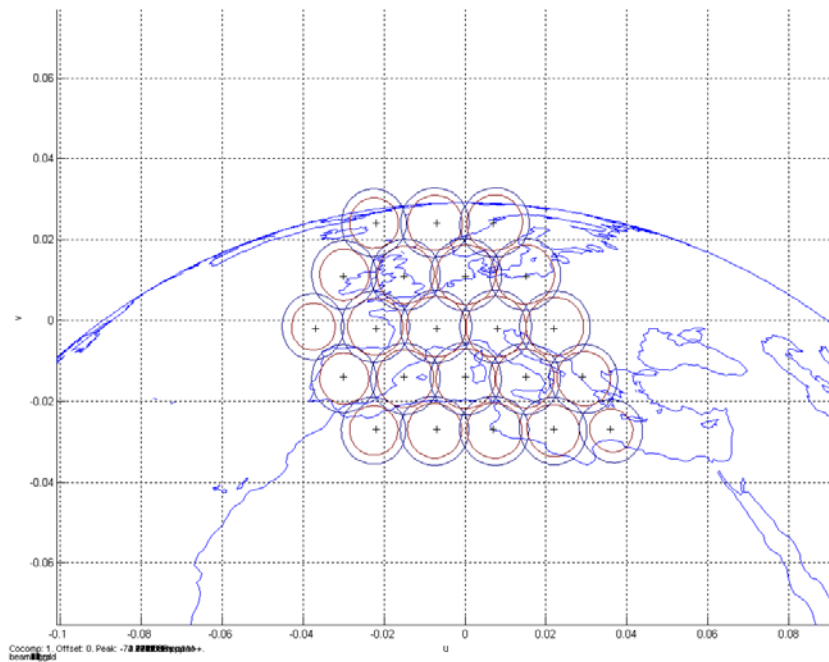


**Figure 6- 3 Beam pattern on the ground**

### 6.3 Frequency Reuse Scheme

Multibeam mobile satellite communication system has the potential to use frequency reuse scheme to improve the system capacity and spectral efficiency. The frequency reuse technique requires low side lobe levels outside the coverage area of each beam. Then it becomes interesting to discover the side lobe levels of the cells with the same frequency. Figure 6-4 shows an example of the contour gain levels of beam 1 and beam 14 which are using the same frequency.

The same frequency cells are plotted to compare the isolation level. The contour levels are from 35 dB to 65 dB and the step size is 5 dB. We will discuss this problem in detail in Chapter 7.

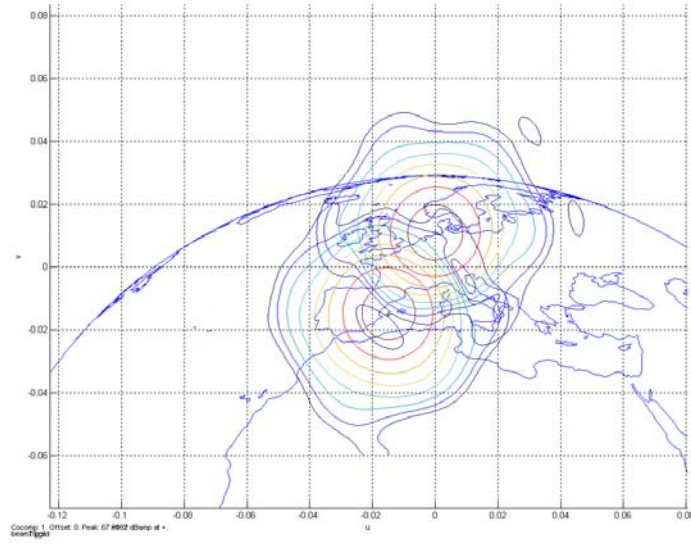


**Figure 6- 4 Contour plot for beam 1 and 14**

# 7 Onboard System Integration

The onboard system consists of the transmitter network and the receiver network. The diplexer serves as a double band pass filter which isolates the transmitter and the receiver. The complete onboard system architecture is shown in Figure 7-1. The band pass filters at the transmitter side will attenuate the inter-modulation products which arise from the power amplifier stage. This allows the nonlinear amplifiers to operate close to saturation for a given output carrier to inter-modulation ratio.

One of the important issues a good designer should remember is that the transmitter network is working at very high power level in order to guarantee the downlink performance while the power received at the receiver network is quite weak due to the high free pass loss. Thus the transmitter power leakage to the receiver side should be considered in order to avoid interference. In order to improve the isolation level between the transmit network and the receive network, additional filters should be placed before the LNA stage.

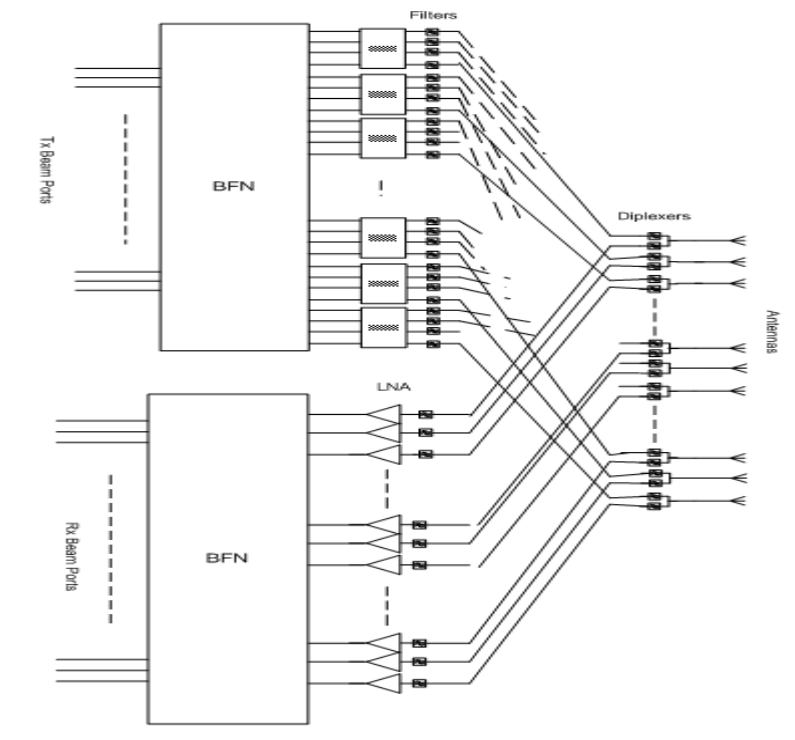
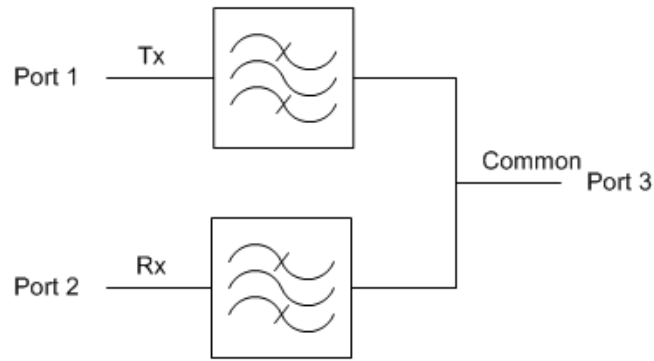


Figure 7- 1 Complete system structure

## 7.1 S matrix for the Diplexer

The diplexer is a three port device. As shown in Figure 7-2, two ports are used to connect the transmit network port and the receive network port. The remaining port which is called common port is used to connect the antenna element.



**Figure 7- 2 Diplexer Structure**

Normally, it is easy to measure the S parameters for a two ports or four ports component. In this manner, the diplexer is measured as a two ports device with the remaining port terminated with a matching load. RUAG Space provided the measured data for Common port to Tx port, Common port to Rx port and Rx port to Tx port. From these measured data, it is desired to build the S matrix for the 3 ports diplexer, which is a 3 by 3 S matrix for a certain frequency. It is expressed as,

$$\begin{bmatrix} S_{TT} & S_{TR} & S_{TC} \\ S_{RT} & S_{RR} & S_{RC} \\ S_{CT} & S_{CR} & S_{CC} \end{bmatrix}$$

For example,  $S_{TR}$  means the transmission coefficient between the transmitter side and the receiver side when the receiver port is excited. The following figures show the property of the diplexer. The horizontal axis is the frequency and the vertical axis is the amplitude in dB unit.

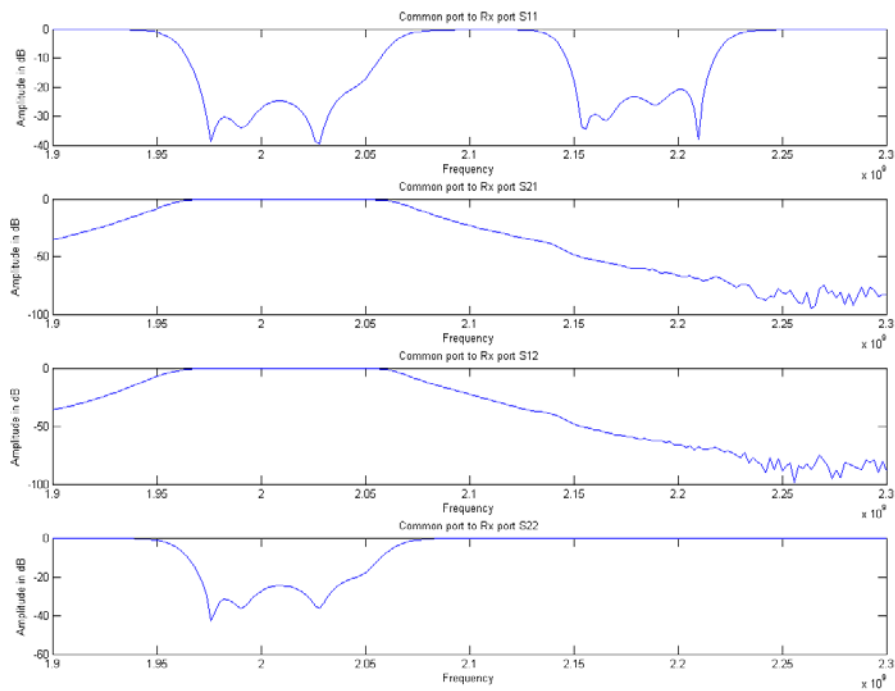


**Figure 7- 3 S parameter of Common port to Rx port**

The measured S parameters from the Common port to the Rx port are shown in Figure 7-3. The first and the fourth sub picture are the reflection coefficients of the common port and the Rx port. The second and the third sub graph are the transmission coefficients from common port to Rx port and from Rx port to common port, respectively. From the figure we can see that the reflection coefficients are below -25 dB at the receive band which is between 1980 MHz and 2025 MHz. The transmission coefficient between the receiver port and the common port is right below 0 dB at the receive band.

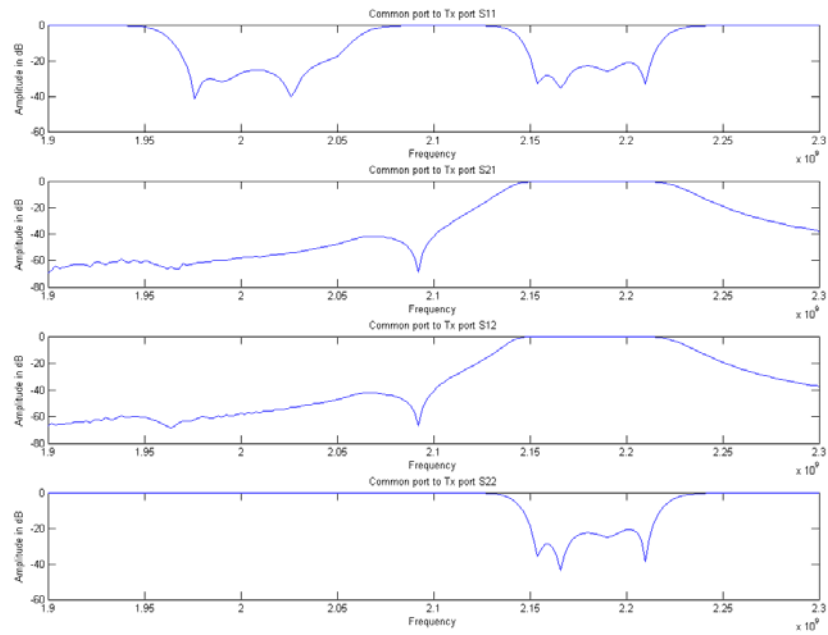


**Figure 7- 4 S parameter of Common port to Tx port**

Compared to Figure 7-3, Figure 7-4 shows the measured S parameters from the Common port to the Tx port. The first and the fourth sub picture are the reflection coefficients of the common port and the Tx port. The second and the third sub graph are the transmission coefficient from common port to Tx port and from Tx port to common port, respectively. This figure shows that the reflection coefficients are below -20 dB at the transmission band which is between 2160 MHz and 2200 MHz. The transmission coefficients between the transmitter port and the common port is right below 0 dB, around -0.3dB to be precise, in the transmission band.

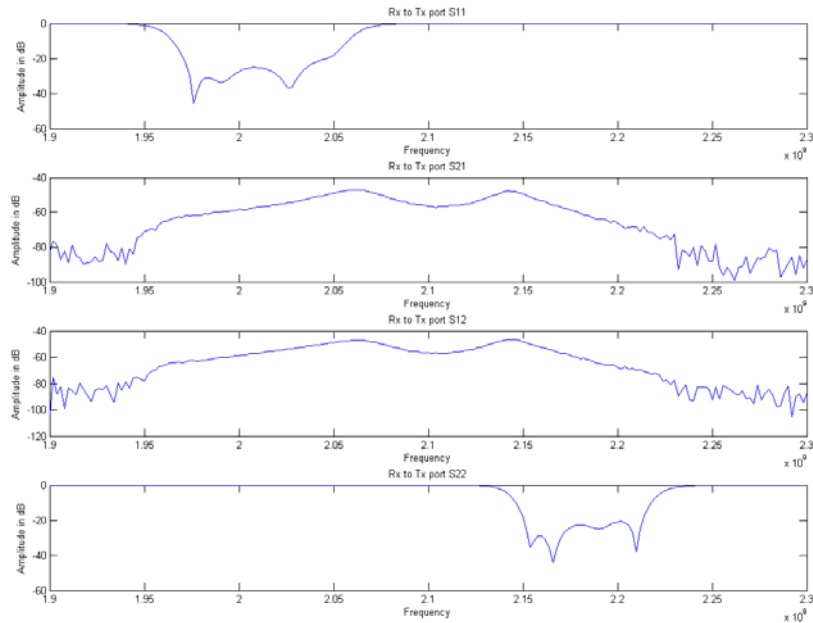


**Figure 7- 5 S parameter of Rx port to Tx port**

Different from the previous two graphs, Figure 7-5 interprets the S parameters between the Tx port and the Rx port. The first and the fourth curves illustrate the reflection coefficient for the transmitter port and the receiver port, respectively. The second and the third curves show the isolation levels between the transmitter side and the receiver side. From these curves we see that the isolation level is below -60 dB at both the transmit and receive bands.

## 7.2 Isolation Level between the Tx Ports and the Rx Ports

We assume the Tx power amplifier gain is 30dB, and we know the path loss of the centre elements of the beamforming network is -9.24 dB and the path loss of the 6 surrounding elements of the beamforming network is -19.24 dB. The receiver LNA gain is 30 dB. In order to check the mutual isolation level between the transmit beam ports and the receive beam ports; we introduced the measured data of the practical diplexer from RUAG Space. According to the antenna specification, the maximum power one antenna element can handle is 100 Watt which is 50 dBm. The measured data of the diplexer shows the isolation between the Tx port and the Rx port is around -60 dB. If the antenna is working at full load, the power leakage to the receiver port is -10dBm. This is much larger than the received signal power from the ground. Thus, additional filtering is needed in order to avoid the inter-modulation interference which arises at the LNA stage.

Additional filters can be added after the BMFA stage at the transmitter side and before the LNA stage at the receiver side to increase the isolation level. These filters are band pass filters which will block the signal from undesired frequencies. At the transmitter side, if filters are added before the diplexer, another problem, the power reflection between the filter and the diplexer, will occur. The designer should take this into account. Another approach is to increase the isolation level at the diplexer stage without introducing another filter. But this scheme will increase the diplexer size and mass. The former scheme can be easily implemented, and the second scheme is not quite

appealing.

### 7.3 Cross Over between the Neighbouring Beams

Seven frequency reuse scheme is quite often used in satellite mobile communication systems. The neighbours do not use the same frequency. However, the interception point of the neighbours is of great interest to evaluate system performance. Figure 7-6 depicts this problem. If users are standing in the red region, they could be serviced from beam 1. In the yellow region, they access service from beam 2 and so on. Then the question becomes what happens to users standing in the white region, which is the interception point of the three neighbours? This question tells us the meaning of evaluating the beam gains on each circle which is the beam coverage edge. By checking the beam gain variations on the circles, the answer can be easily obtained.

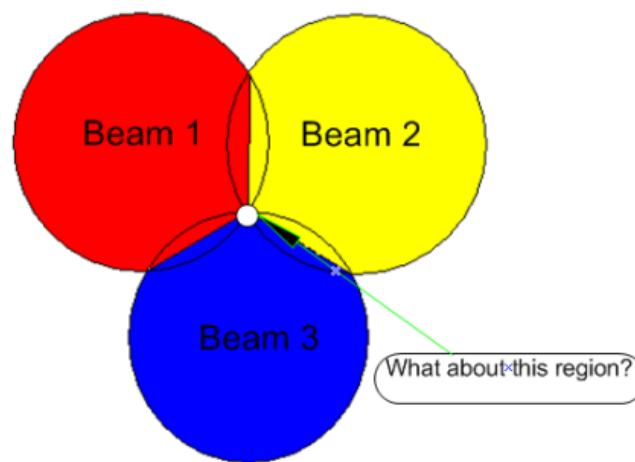


**Figure 7- 6 Beam crossover**

Before deciding which service cell the user belongs to, we need to calculate the distance between the beam centre and the interception point first. Figure 7-7 shows the simulation results of three neighbouring beams; beam no12, 13 and 17. The working frequency is 2180MHz which is the centre frequency of the transmit band. These three beams form a rotated triangle just as shown in Figure 7-6. The contour levels are 64 dBi and 65 dBi. Figure 7-8, 7-9 and 7-10 illustrate the gain contour levels of beams 12, 13 and 17, from 60 dBi to 65 dBi. The small green circles are the evaluation points.

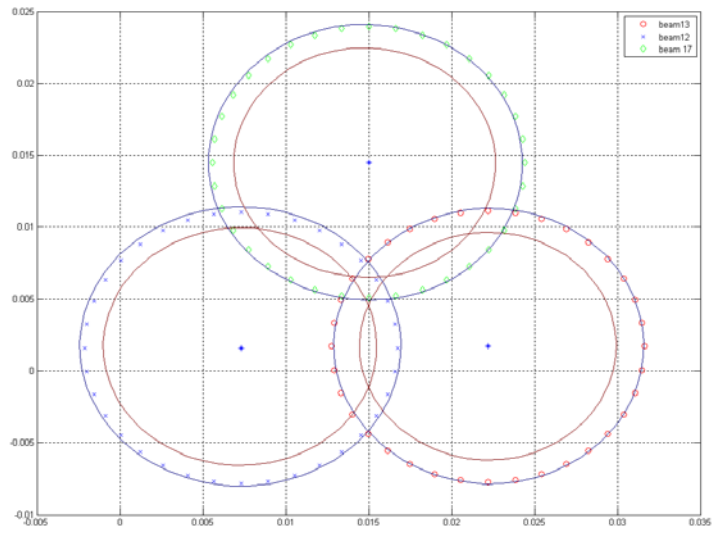


**Figure 7- 7 Beam pattern for beam 12, 13 and 17**

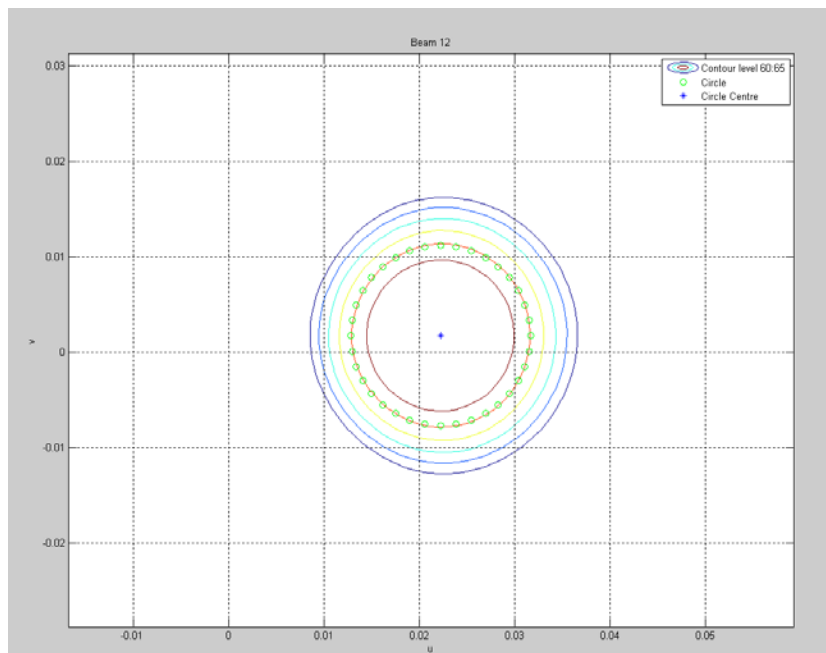


**Figure 7- 8 Beam pattern for beam 12**

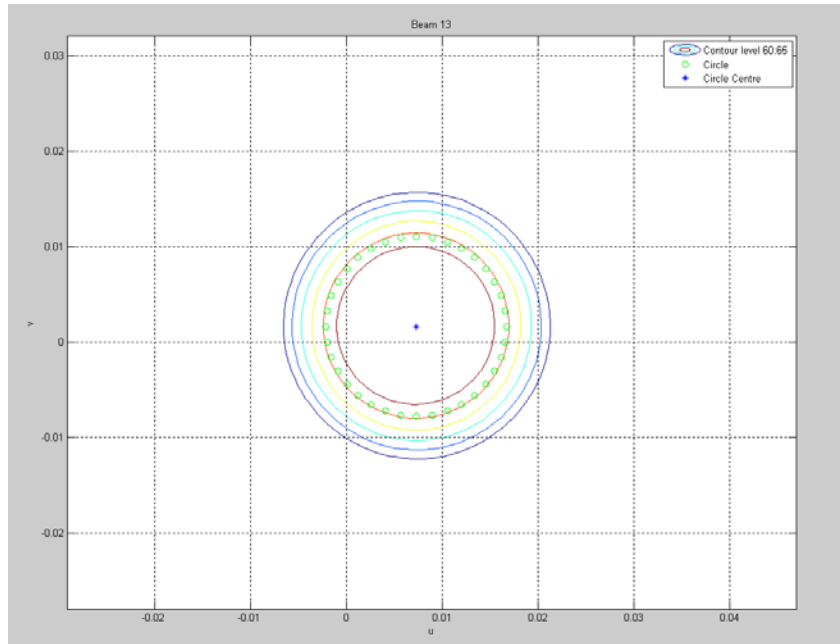


**Figure 7- 9 beam pattern for beam 13**

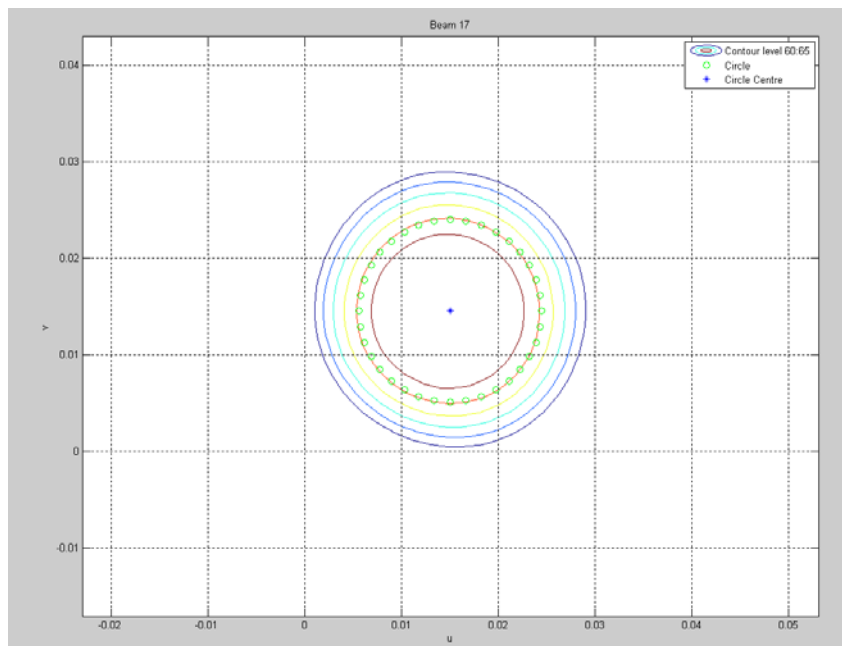


**Figure 7- 10 Beam pattern for beam 17**

Figure 7-8, 7-9 and 7-10 show the beam pattern for the three neighbouring beams in the UV coordinates. The horizontal axis is the U coordinate and the vertical axis is the V coordinate. The area in the small green circles stands for the coverage area for each beam and the blue star is the centre position of the corresponding beam. These figures show the beam gain on the edge of these beams are around 64 dBi with small variations. The smaller the variations are the better service a user can obtain at the beam coverage edge.

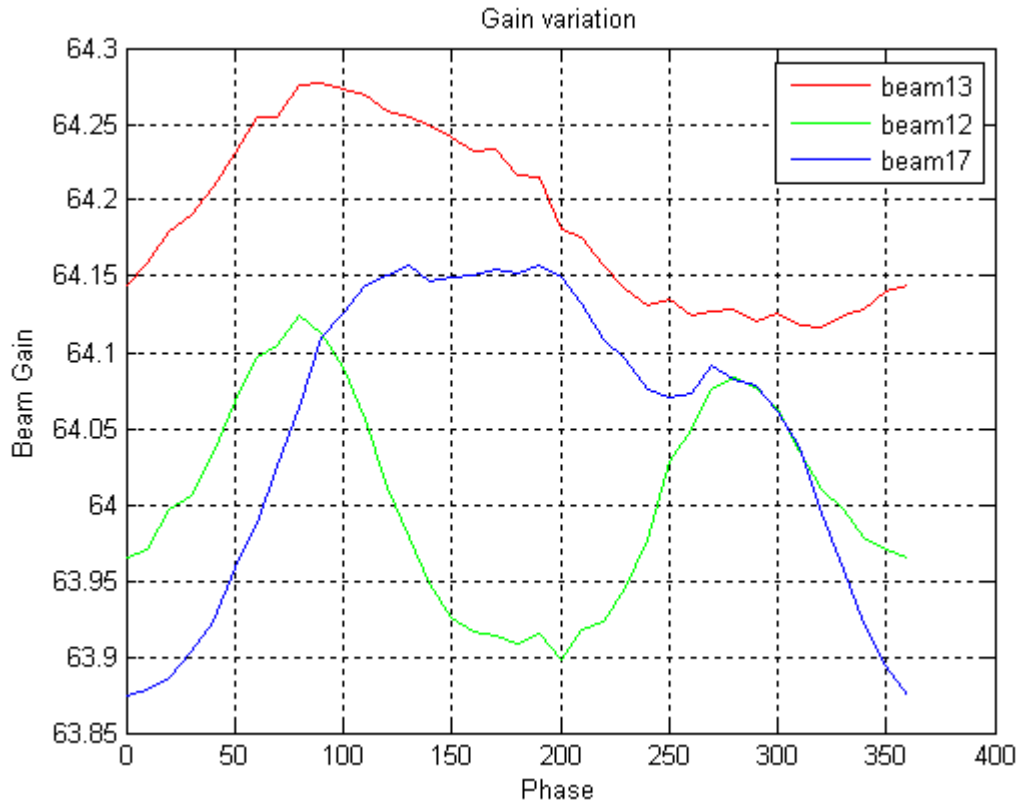


**Figure 7- 11 Beam coverage edge gain variations without error vectors**

Figure 7-11 shows the gain variations on the evaluation points of the three beams. The horizontal axis shows the phases along the edge of the coverage area on Figure 7-7, 7-8 and 7-9 and the vertical axis shows the beam gain variations on the coverage edges. We can see the interception point for beam 13 is located at 135 degree approximately. The gain at this angle is 64.23 dBi as shown in Figure 7-11. The interception point for beam 12 and beam 17 are located at 45 and 90 degree, which corresponding to beam gain 64.03dBi and 64.07 dBi, respectively. Therefore, beam 13 has a better beam gain compared to the other two. Users in this interception region can choose the service from beam 13. This figure also illustrates the maximum gain variations for beams 13, 12 and 17, that are 0.1602 dB, 0.2261 dB and 0.2834 dB to be exact.

## 7.4 Error Vectors for the Transmitter Network

The previous section shows the gain variations on the beam coverage edges and the service selection for the three neighbouring beams. However, the amplitude and phase of the signal can be affected by the manufacturing errors, operating power levels or the material property of the components. This introduces the need to employ error vectors to each component. Our simulations are based on scattering parameters. Thus the error vectors are square matrixes with the reflection coefficients errors on the main diagonal and the transmission coefficients errors off the diagonal. These error vectors will help us to analyze the tolerance for each component. As the first approach, we assume the error vector for each component is normal distribution with a certain mean value and standard deviation. The tricky part is the phase distribution of the reflection coefficients. Since

it could be any angle between 0 to 2 pi, we assume it is a uniform distribution between 0 to 2 pi. We can start with some practical data for evaluating the system. The first assumption for the error vector is that the mean amplitude of the reflection coefficients of the each component is -20dB and the standard deviation is 2dB, the mean amplitude of the transmission coefficients of each component is 0 dB and the standard deviation is 0.1dB. The phase distribution of the transmission coefficients can be treated as a normal distribution with mean value 0 and standard deviation 2 degrees.

### 7.4.1 Test Methodology

The system tolerance simulations are based on the error vectors for each component as well as the complete system.

Firstly, we need to choose the criteria for our measurement. A reasonable assumption is that the gain variations on the beam coverage edge should not exceed 0.5 dB for a single stage test and 1 dB for the system level test. The single stage test means we introduce the error vector to the BFN, the Butler matrix and the HPAs stage by stage. When the BFN is tested, the rest of the components such as the Butler matrixes and the HPAs are error free. The system level test means all the components in the transmitter network are added with error vectors.

Secondly, we can start to test the single stage tolerance based on the gain variation (0.5 dB) mentioned before. If the error vector causes the gain variation larger than 0.5 dB, we need to stop increasing errors.

Thirdly, error vector for all the components should be added based on the values obtained from step 2. If the system works properly under such a condition, we can increase the system tolerance by adding even larger errors. Otherwise, we need to decrease the error tolerance.

When the phase deviation of the transmission coefficient has been increased to 5 degrees and the system performance is still acceptable, we can start to increase the amplitude deviation to find its limit. The reason is that 5 degrees corresponding to 1.1mm in manufacture mismatch length for transmit centre frequency (2180MHz), according to Equation (7.1). The current manufacture technology can easily fulfil this requirement.

$$L = \frac{C}{\sqrt{\epsilon_r} f} \frac{PhaseDeviation}{360} \quad (7.1)$$

Here, L stands for the deviation in length, C means the light speed,  $\epsilon_r = 2.94$  is the dielectric constant and f is the working frequency.

### 7.4.2 Simulation Results

#### Beamforming Network Analysis:

First, let us start with beam forming network analysis. The following values are for the error vectors. The first assumption is that the mean value for the reflection coefficients is -20 dB (Sii\_errorMean) with 2 dB standard deviation (Sii\_errorSTD). The phase distribution for the reflection coefficients is uniformly distributed between 0 and 2 pi. The mean value for the transmission coefficients error is 0 dB with 0.1 dB standard deviation (Sij\_errorSTD). The phase

distribution is a normal distribution with 0 mean and 2 degrees deviation ( $S_{ii\_errorPhase\_STD}$ ). The result is shown in Figure 7-12.

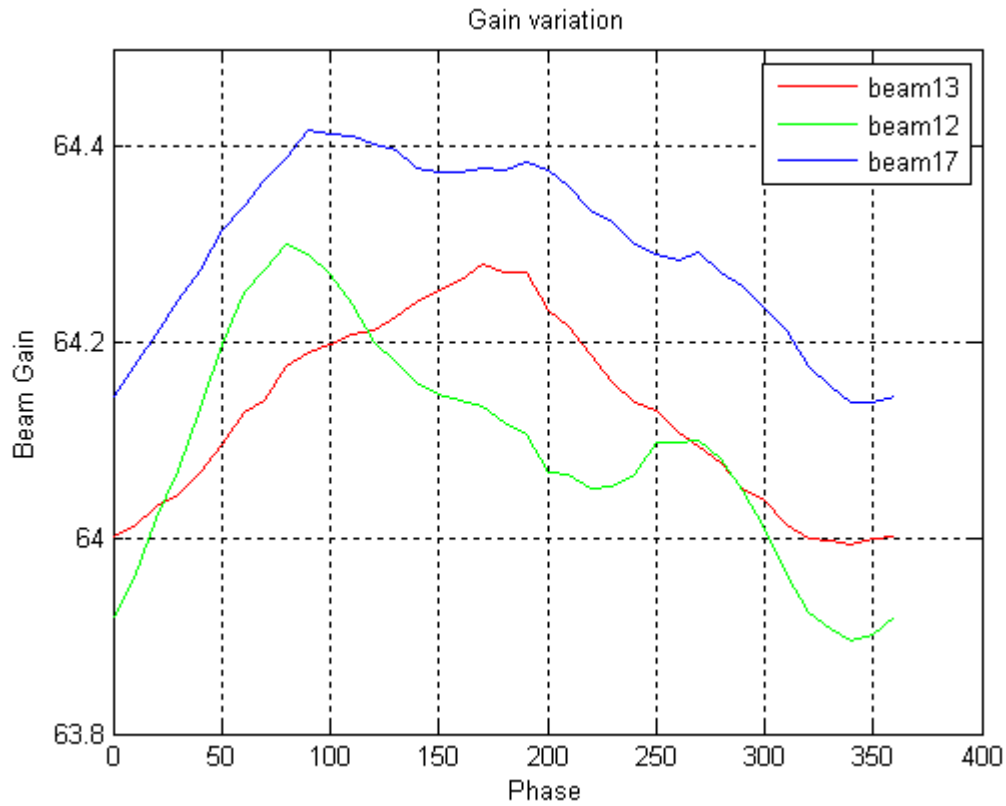
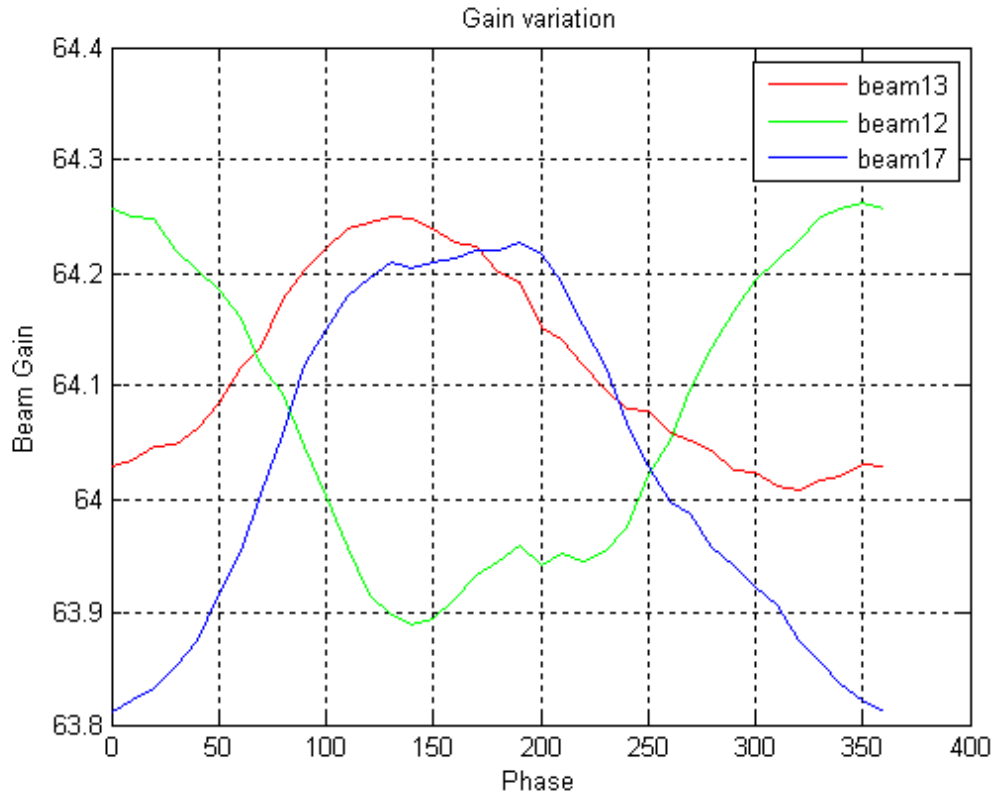


Figure 7- 12 Beam coverage edge gain variations when  $S_{ii\_errorMean} = -20\text{dB}$ ,  $S_{ii\_errorSTD} = 2\text{dB}$  and  $S_{ij\_errorSTD} = 0.1\text{dB}$ ,  $S_{ij\_errorPhase\_STD} = 2$  degrees

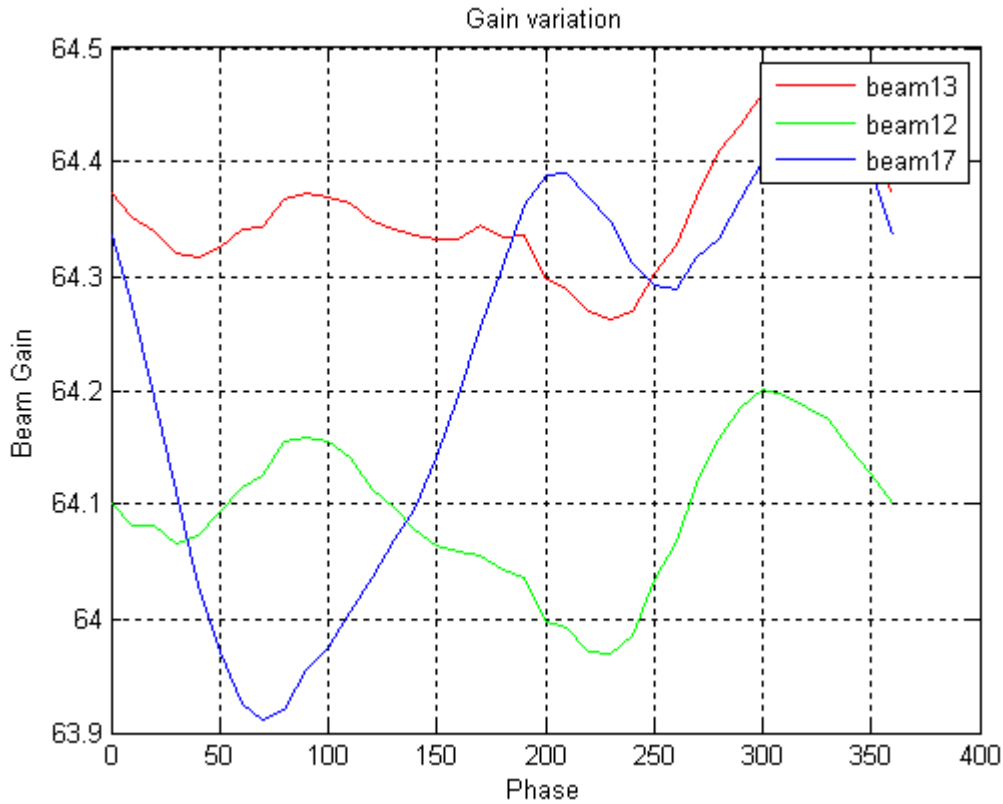
Figure 7-12 shows the variations for beam 12, 13, and 17 are 0.4 dB, 0.29 dB and 0.28 dB, respectively. These results show that the system works properly under the first assumption. Thus, we can start to increase the errors.

We increase the transmission amplitude deviation to 0.17dB. The result is shown in Figure 7-13.



**Figure 7- 13 Beam coverage edge gain variations when  $S_{ii\_errorMean} = -20\text{dB}$ ,  $S_{ii\_errorSTD} = 2\text{dB}$  and  $S_{ij\_errorSTD} = 0.17\text{dB}$ ,  $S_{ij\_errorPhase\_STD} = 2$  degrees**

In this case, the gain variations increased to 0.34 dB, 0.38 dB and 0.42 dB corresponding to beam 12, 13 and 17. The performance is still acceptable. Then we could start to increase the transmission coefficients phase deviation to 5 degrees. The result is shown in Figure 7-14.



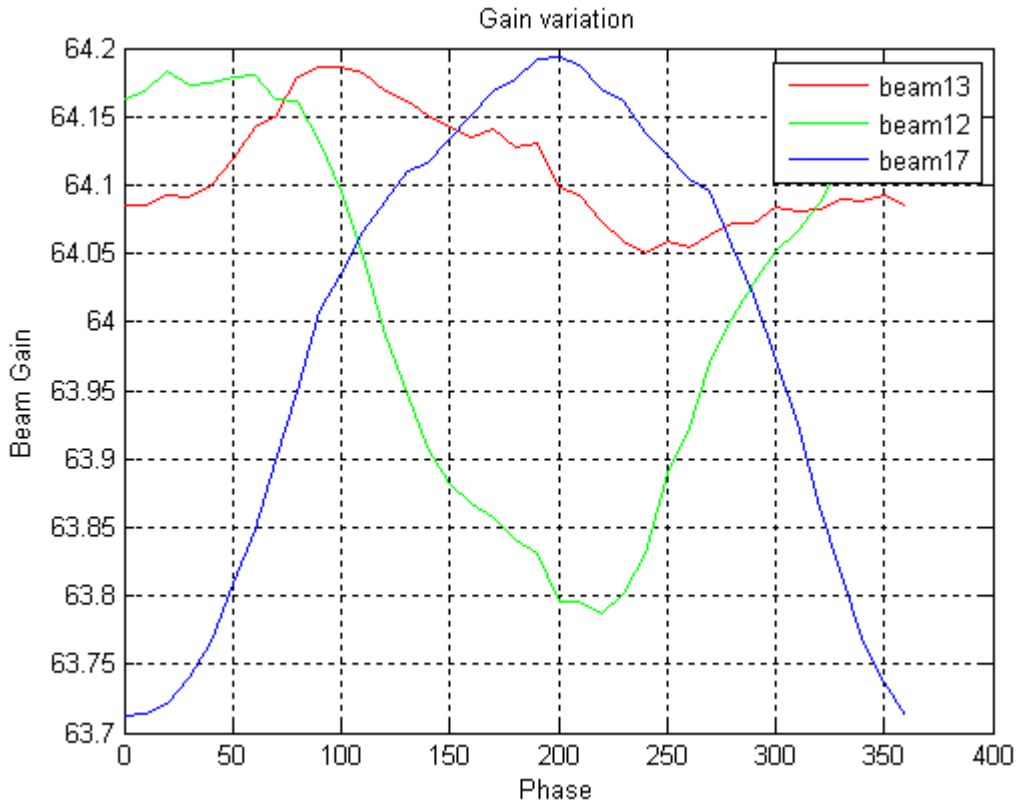
**Figure 7- 14 Beam coverage edge gain variations when  $S_{ii\_errorMean} = -20\text{dB}$ ,  $S_{ii\_errorSTD} = 2\text{dB}$  and  $S_{ij\_errorSTD} = 0.17\text{dB}$ ,  $S_{ij\_errorPhase\_STD} = 5$  degrees**

Figure 7-14 shows that the gain variations exceed 0.5 dB for beam 17, which means that the 5 degrees phase error is unacceptable. Because the errors are random, more simulations can be performed to obtain the average results. Table 7-1 shows the simulation results for this error vector after simulating three independent realizations of the errors.

**Table 7- 1**

| Beam Number/ Error realization | Beam 12 | Beam 13 | Beam 17 |
|--------------------------------|---------|---------|---------|
| 1                              | 0.34    | 0.38    | 0.42    |
| 2                              | 0.51    | 0.46    | 1.12    |
| 3                              | 0.45    | 0.5     | 0.52    |
| Average                        | 0.43    | 0.47    | 0.69    |

Some values in Table 7-1 are larger than 0.5 dB, and the average variation of beam 17 is still larger than 0.5 dB. For this reason, we need to back up to 3 degrees phase deviation. The results are shown in Figure 7-15.



**Figure 7- 15 Beam coverage edge gain variations when  $S_{ii\_errorMean} = -20\text{dB}$ ,  $S_{ii\_errorSTD} = 2\text{dB}$  and  $S_{ij\_errorSTD} = 0.17\text{dB}$ ,  $S_{ij\_errorPhase\_STD} = 3$  degrees**

The gain variation for beam 17 is just below the system tolerance. Since the error vectors are random, the average results are more reliable. Table 7-2 shows that the average results are below 0.5 dB and no value in the table is larger than 0.5 dB. Therefore, if the system is to work properly most of the time (99%), the transmission amplitude deviation should not exceed 0.17 dB; say 0.15 dB deviation could be the system specification. The phase deviation should not exceed 3 degrees.

**Table 7- 2**

| Beam Number/ Error realization | Beam 12 | Beam 13 | Beam 17 |
|--------------------------------|---------|---------|---------|
| 1                              | 0.4     | 0.18    | 0.45    |
| 2                              | 0.4     | 0.17    | 0.48    |
| 3                              | 0.49    | 0.23    | 0.42    |
| Average                        | 0.43    | 0.19    | 0.45    |

In summary, for the beamforming network, a component with -20 dB reflection coefficients error (2 dB deviation), and 0 dB transmission coefficients error (0.15 dB amplitude deviation and 3 degrees deviation) is acceptable.

### Left Hand Butler Matrix Analysis:

-20 dB reflection coefficients with 2 dB standard deviations and 0 dB mean value for transmission coefficients error with 0.1 dB standard deviations can be the first assumption. The phase deviations for transmission coefficients are 2 degrees. The result is shown in Figure 7-16.

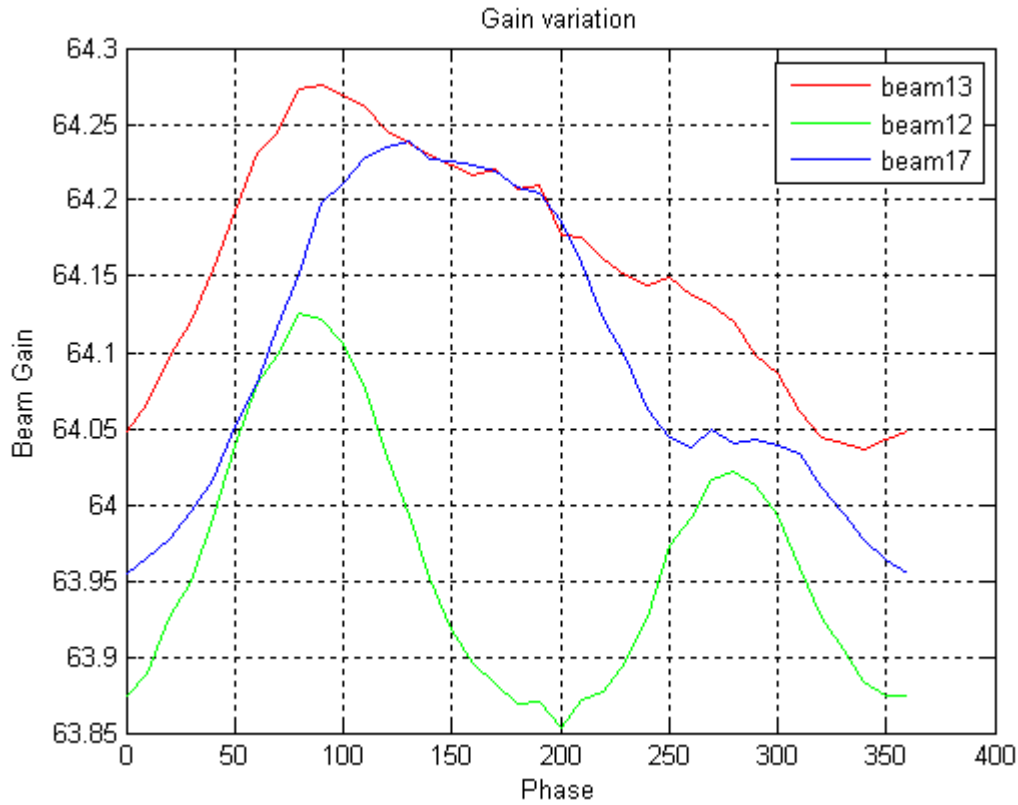


**Figure 7- 16 Beam coverage edge gain variations when  $S_{ii\_errorMean} = -20dB$ ,  $S_{ii\_errorSTD} = 2dB$  and  $S_{ij\_errorSTD} = 0.1dB$ ,  $S_{ij\_errorPhase\_STD} = 2$  degrees**

The gain variations for the three beams keep below 0.5 dB. Then the errors can be increased step by step. When the transmission coefficients amplitude error increased to 0.67 dB with 5 degrees phase errors, the gain variation for beam 12 exceeds 0.5dB. The result is shown in Figure 7-17. Table 7-3 shows the simulation results in three independent realizations. The average results are below 0.5 dB. Sometimes, however, the gain variations exceed the system tolerance.

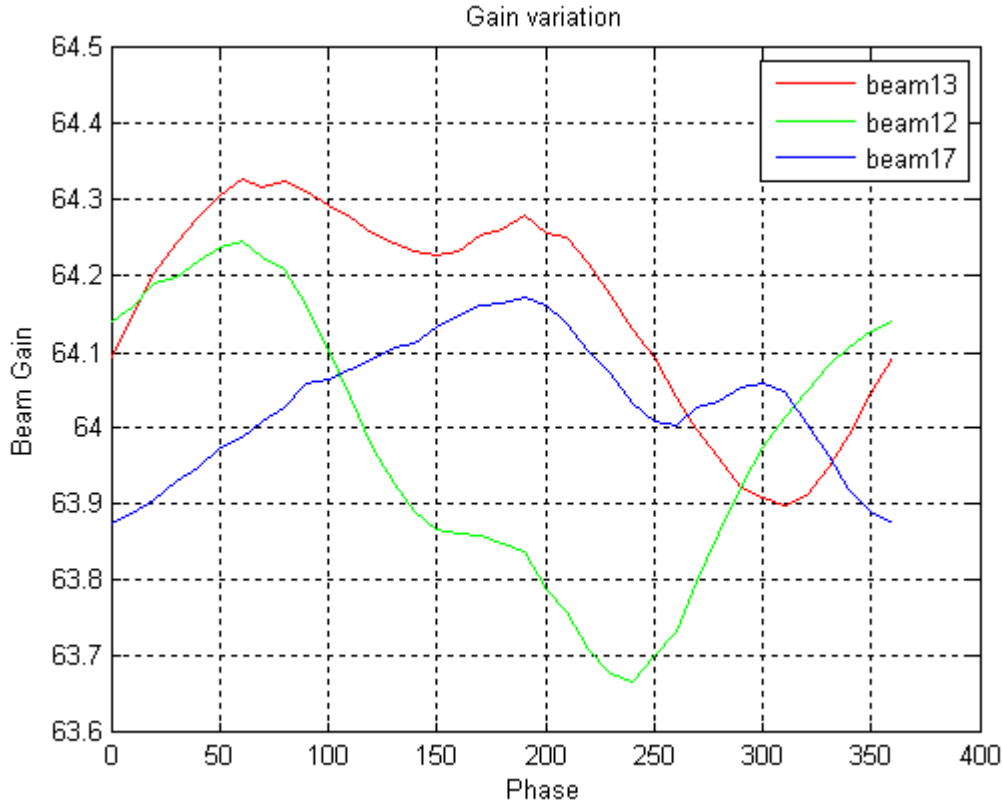


**Figure 7- 17 Beam coverage edge gain variations when  $S_{ii\_errorMean} = -20\text{dB}$ ,  $S_{ii\_errorSTD} = 2\text{dB}$  and  $S_{ij\_errorSTD} = 0.67\text{dB}$ ,  $S_{ij\_errorPhase\_STD} = 5$  degrees**

**Table 7- 3**

| Beam Number/ Error realization | Beam 12 | Beam 13 | Beam 17 |
|--------------------------------|---------|---------|---------|
| 1                              | 0.56    | 0.42    | 0.29    |
| 2                              | 0.23    | 0.49    | 0.37    |
| 3                              | 0.47    | 0.31    | 0.35    |
| Average                        | 0.42    | 0.41    | 0.34    |

To sum up, the requirements for the left hand butler matrix could be -20 dB reflection coefficients with 2 dB deviation. The transmission coefficients tolerance could be 0.6 dB in amplitude and 5 degrees in phase.

**Power Amplifier Analysis:**

The signal is working at lower power level before this stage, but at this stage, the signal will be amplified and become loss sensitive. The first assumption can be the same as before and the result is shown in Figure 7-18.

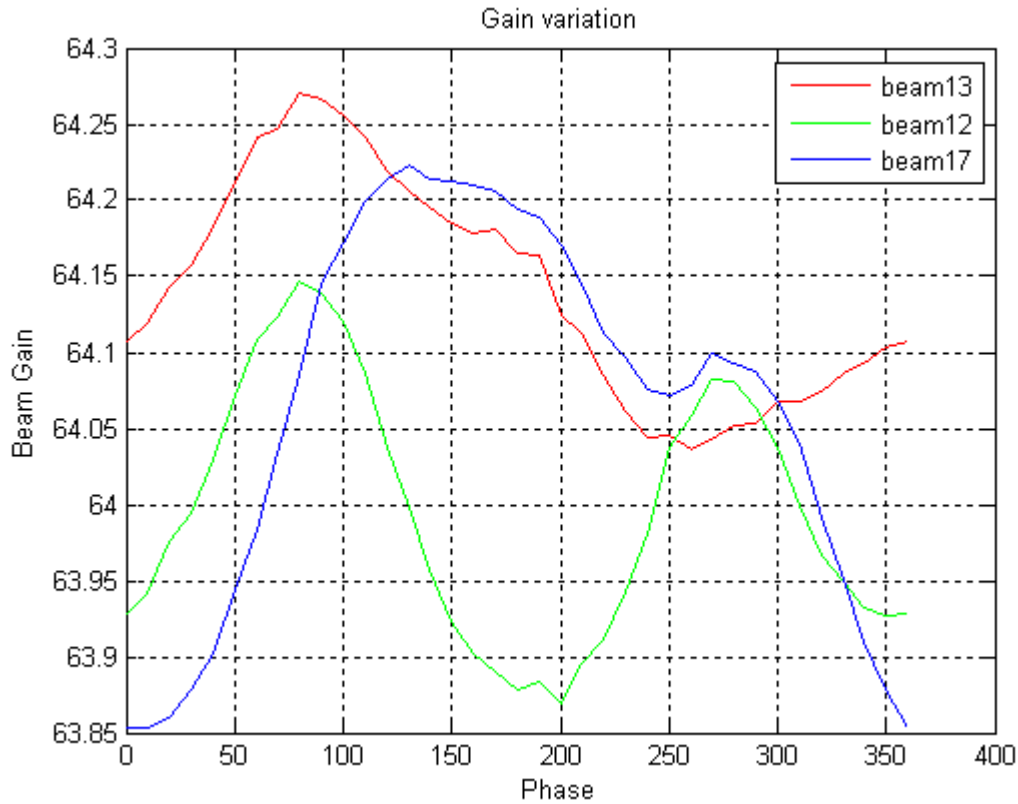


**Figure 7- 18 Beam coverage edge gain variations when  $S_{ii\_errorMean} = -20\text{dB}$ ,  $S_{ii\_errorSTD} = 2\text{dB}$  and  $S_{ij\_errorSTD} = 0.1\text{dB}$ ,  $S_{ij\_errorPhase\_STD} = 2$  degrees**

Figure 7-18 shows that the gain variations are still far below 0.5dB. When the phase deviation increased to 5 degrees and the amplitude deviation increased to 0.42 dB, the gain variation of beam 13 is larger than 0.5dB which is shown in Figure 7-19. Table 7-4 shows that the average results are below 0.5 dB in this specification. But the gain variations for beam 13 and 17 are larger than 0.5 dB occasionally.

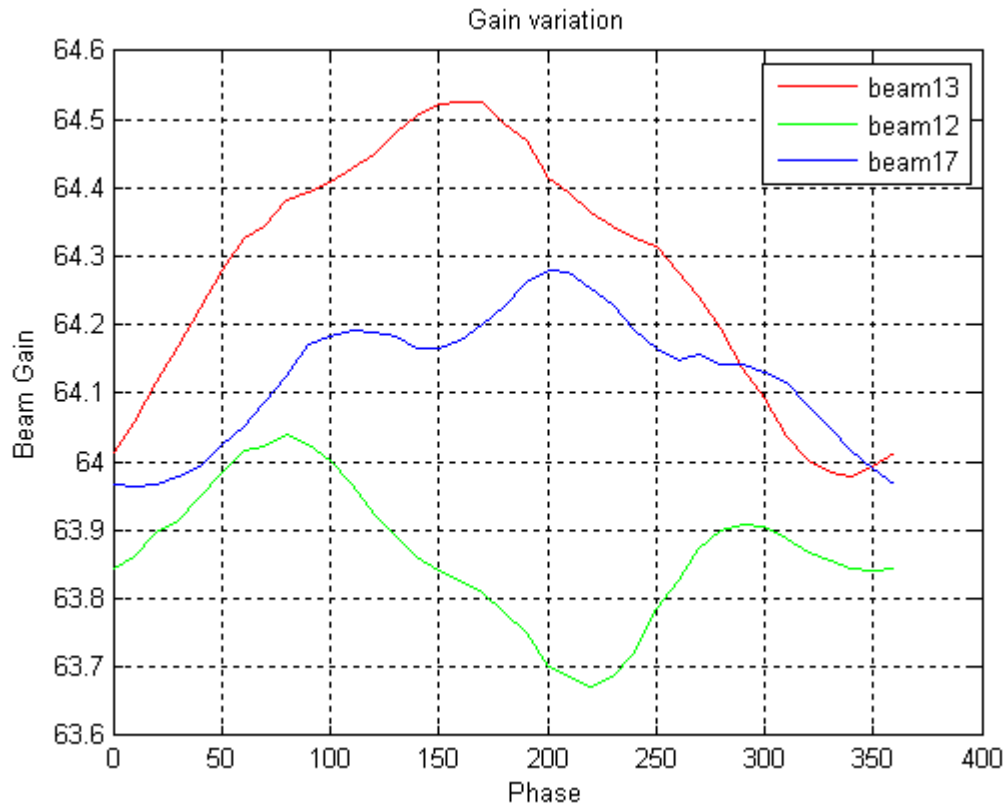


**Figure 7- 19 Beam coverage edge gain variations when  $S_{ii\_errorMean} = -20\text{dB}$ ,  $S_{ii\_errorSTD} = 2\text{dB}$  and  $S_{ij\_errorSTD} = 0.42\text{dB}$ ,  $S_{ij\_errorPhase\_STD} = 5$  degrees**

**Table 7- 4**

| Beam Number/ Error realization | Beam 12 | Beam 13 | Beam 17 |
|--------------------------------|---------|---------|---------|
| 1                              | 0.34    | 0.54    | 0.31    |
| 2                              | 0.43    | 0.47    | 0.36    |
| 3                              | 0.34    | 0.35    | 0.57    |
| Average                        | 0.37    | 0.45    | 0.41    |

In sum, the transmission coefficients amplitude deviation should be kept below 0.4 dB and the phase deviation can reach up to 5 degrees.

**Right Hand Butler Matrix Analysis:**

The first assumption could be the same as before. And the gain variations are below 0.5dB which is shown in Figure 7-20.

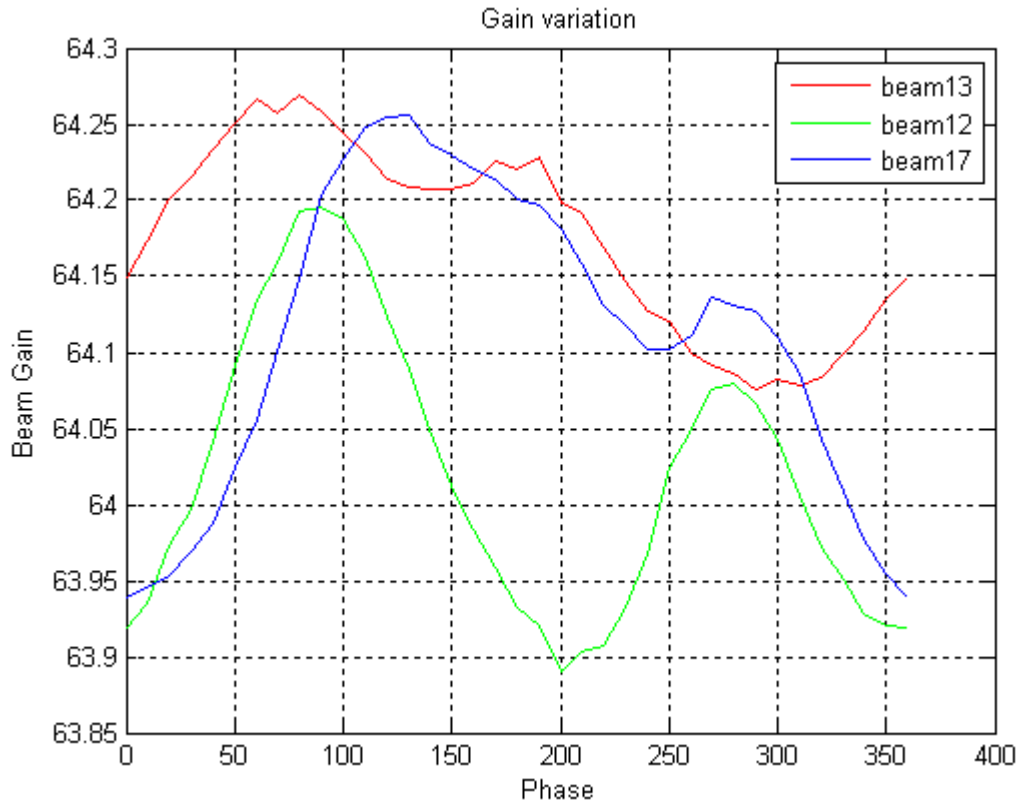


**Figure 7- 20 Beam coverage edge gain variations when  $S_{ii\_errorMean} = -20\text{dB}$ ,  $S_{ii\_errorSTD} = 2\text{dB}$  and  $S_{ij\_errorSTD} = 0.1\text{dB}$ ,  $S_{ij\_errorPhase\_STD} = 2$  degrees**

When the phase deviation is increased to 5 degrees and the amplitude deviation is increased to 0.42 dB, the gain variation of beam 13 is larger than 0.5dB which is shown in Figure 7-21. The average results of three realizations are below 0.5 dB as shown in Table 7-5. Sometimes, however, the gain variations exceed the system tolerance.

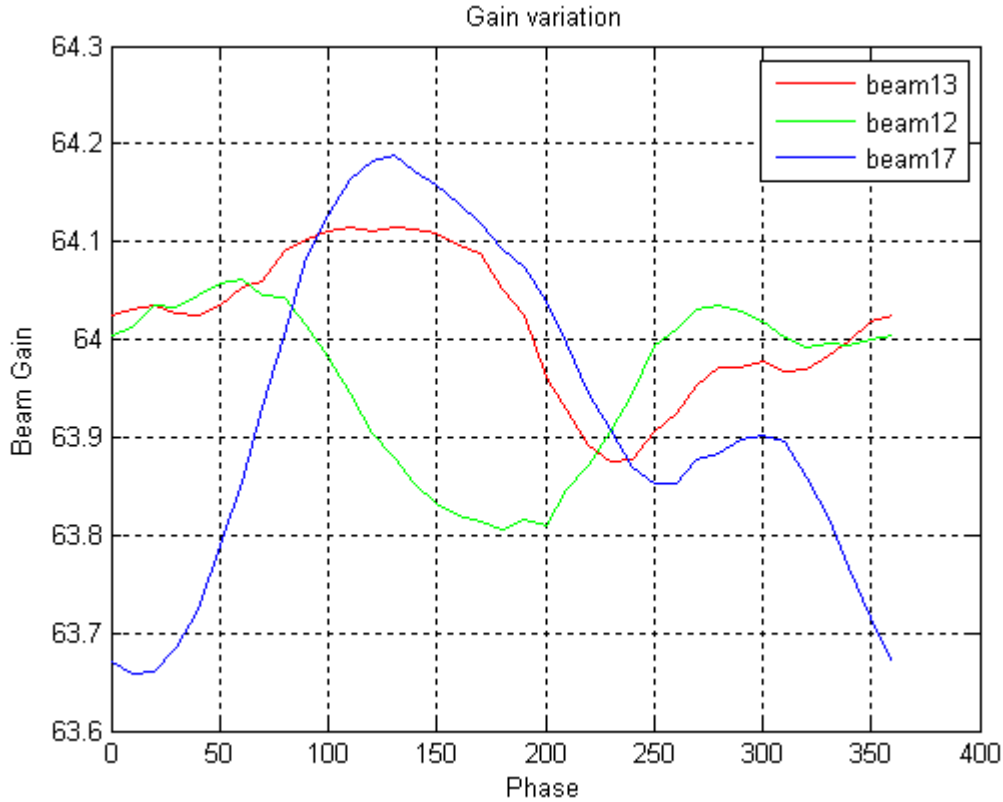


**Figure 7- 21 Beam coverage edge gain variations when  $S_{ii\_errorMean} = -20\text{dB}$ ,  $S_{ii\_errorSTD} = 2\text{dB}$  and  $S_{ij\_errorSTD} = 0.42\text{dB}$ ,  $S_{ij\_errorPhase\_STD} = 5$  degrees**

**Table 7- 5**

| Beam Number/ Error realization | Beam 12 | Beam 13 | Beam 17 |
|--------------------------------|---------|---------|---------|
| 1                              | 0.24    | 0.24    | 0.5     |
| 2                              | 0.51    | 0.33    | 0.13    |
| 3                              | 0.48    | 0.41    | 0.41    |
| Average                        | 0.41    | 0.33    | 0.35    |

To sum up, we can see that the beamforming network needs to be well manufactured to fulfil the specification. The right hand butler matrixes and the power amplifiers should be much more accurate than the left hand butler matrixes. In consequence, we need to place much more accurate components at the high power stages.

**System Analysis:**

The former section shows the requirements for individual components at the transmitter side. Then what will happen if all the components are adding their own error vectors? The first test case is a mean value of -20 dB reflection coefficient with 2 dB standard deviation. The transmission coefficients amplitude error mean value is 0 dB with 0.1 dB standard deviation. The phase error

for the transmission coefficients is 2 degrees. In this way, all the components in the transmitter side have the same error vector. The tolerance for the beam gain variation is set to 1dB. The result is shown in Figure 7-22.

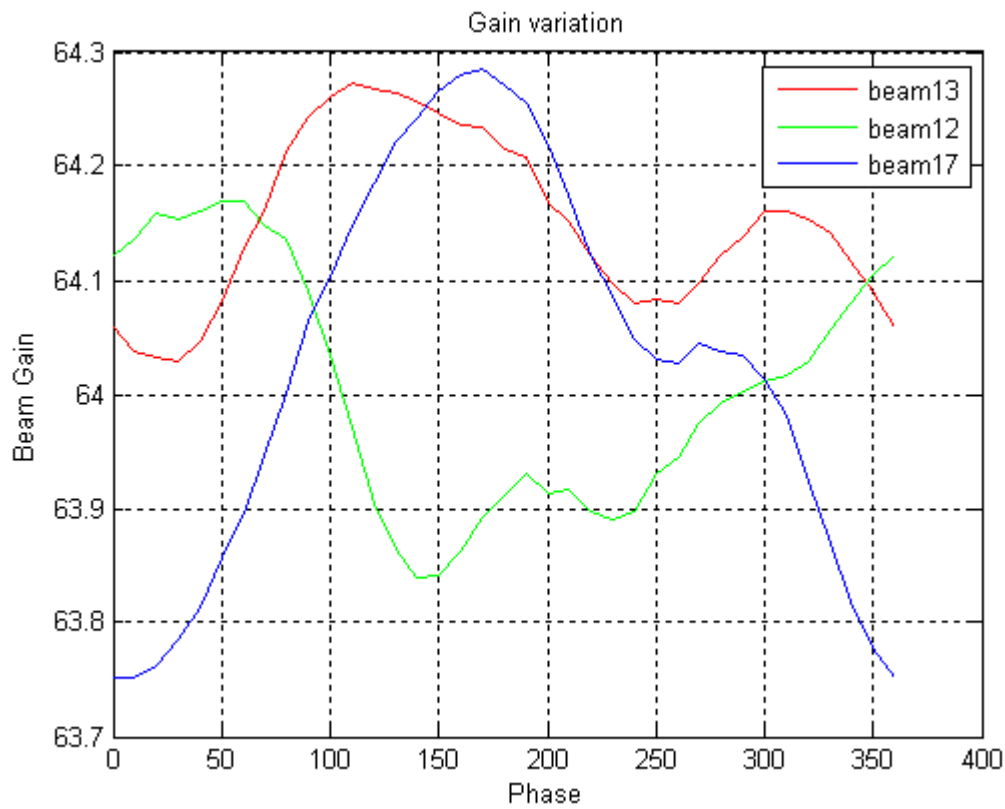


**Figure 7- 22 Beam coverage edge gain variations when  $S_{ii\_errorMean} = -20\text{dB}$ ,  $S_{ii\_errorSTD} = 2\text{dB}$  and  $S_{ij\_errorSTD} = 0.1\text{dB}$ ,  $S_{ij\_errorPhase\_STD} = 2$  degrees**

Figure 7-22 shows that the gain variations are far below the 1 dB tolerances. Thus, even larger errors can be added in the system. The system performance starts to deteriorate when the transmission coefficient amplitude and phase standard deviation are increased to 0.25dB and 5 degrees while the reflection coefficients remain the same. The result is shown in Figure 7-23.

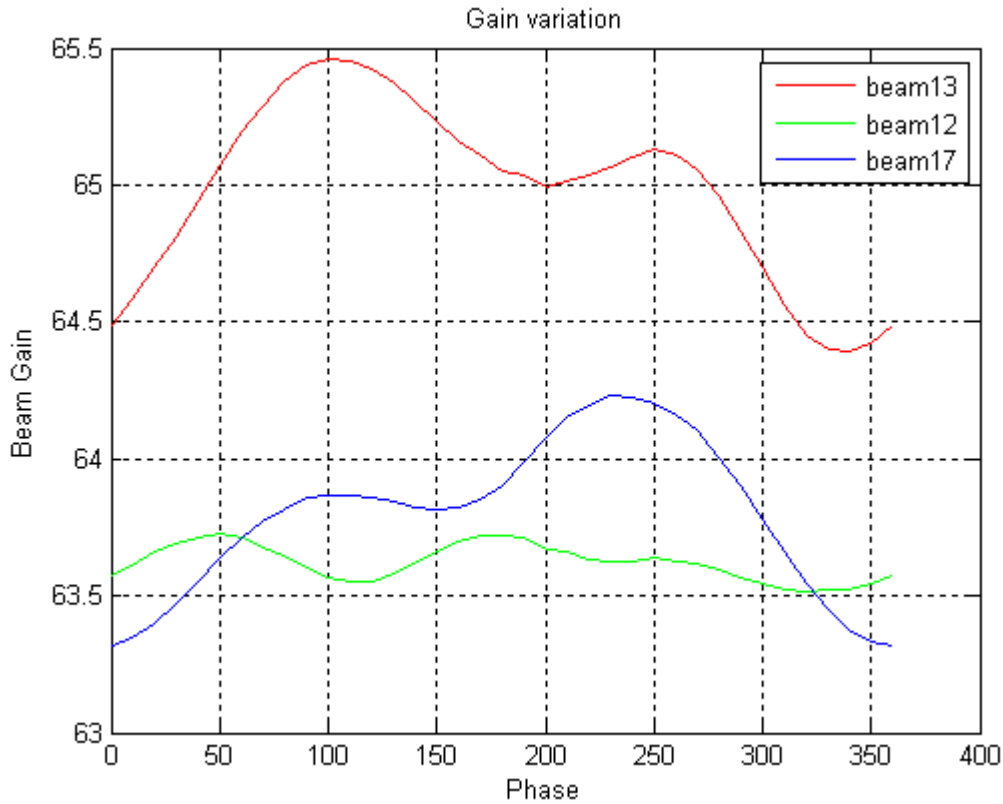


**Figure 7- 23 Beam coverage edge gain variations when  $S_{ii\_errorMean} = -20\text{dB}$ ,  $S_{ii\_errorSTD} = 2\text{dB}$  and  $S_{ij\_errorSTD} = 0.25\text{dB}$ ,  $S_{ij\_errorPhase\_STD} = 5$  degrees**

The gain variation for beam 13 is larger than 1 dB which is not acceptable. Table 7-6 shows that some of the gain variations always larger than 1 dB in every simulation. Thus, the system can not tolerate this level of errors.

**Table 7- 6**

| Beam Number/ Error realization | Beam 12 | Beam 13 | Beam 17 |
|--------------------------------|---------|---------|---------|
| 1                              | 0.25    | 1.02    | 0.85    |
| 2                              | 1.03    | 0.59    | 1.1     |
| 3                              | 1.08    | 0.61    | 0.49    |
| Average                        | 0.79    | 0.74    | 0.81    |

All in all, the system specification for all the components could be: the reflection coefficients' mean value is -20 dB with 2 dB deviations and the transmission coefficients' amplitude standard deviation is 0.2dB with 5 degree phase deviation. This is just one suggestion for the components' specifications. The simulation results of each component show which component is the most error sensitive. Thus we can choose different combinations for different components with different specifications. For example, the reflection coefficients requirement could be a normal distribution

with mean of -20 dB and 2 dB standard deviation. The transmission coefficients amplitude standard deviation errors for BFN, left hand Butler matrix, power amplifiers, and right hand butler matrix can be 0.17 dB, 0.42 dB, 0.25dB and 0.25 dB, respectively. The phase errors for the transmission coefficients are set to 5 degrees for all the components. The simulation results show that the system works properly in this combination, which is shown in Figure 7-24.

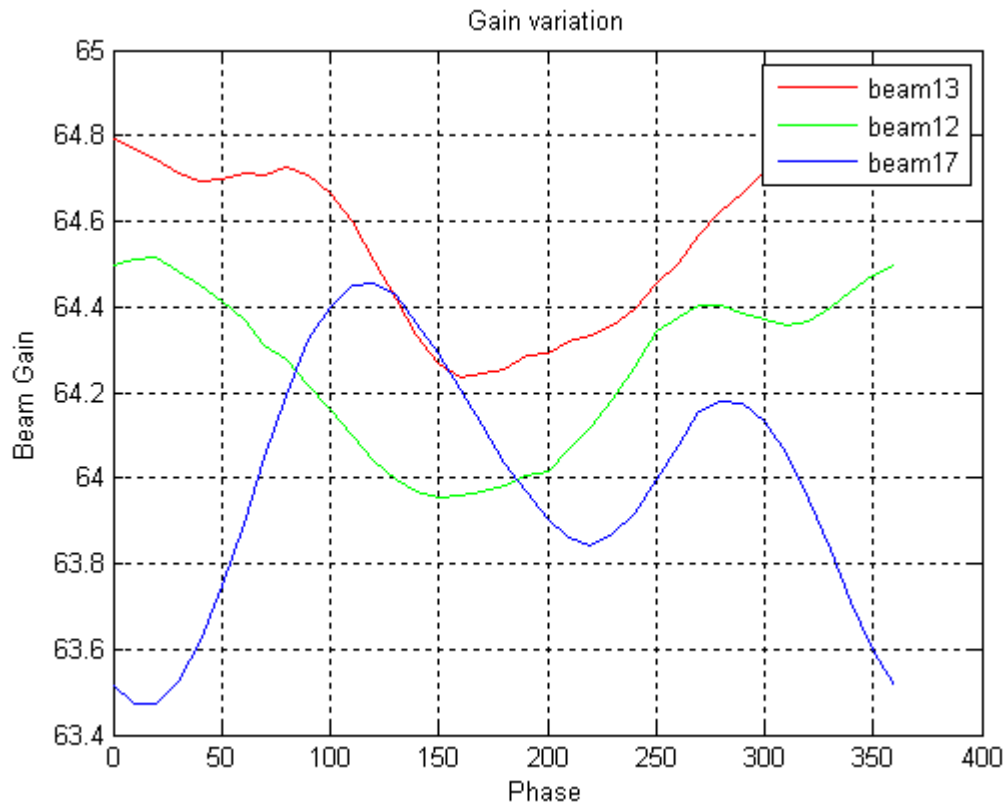


**Figure 7- 24 Beam coverage edge gain variations for a sample combination**

Table 7-7 illustrates the simulation results for three iterations. In most of the time, the system works properly.

**Table 7- 7**

| Beam Number/ Error realization | Beam 12 | Beam 13 | Beam 17 |
|--------------------------------|---------|---------|---------|
| 1                              | 0.55    | 0.56    | 0.95    |
| 2                              | 0.92    | 0.39    | 1.0     |
| 3                              | 0.26    | 0.25    | 0.76    |
| Average                        | 0.58    | 0.4     | 0.903   |

## 7.5 Frequency Reuse (Side Lobe Level Measurement)

A frequency reuse scheme can be used to improve the system capacity and spectral efficiency. The multibeam mobile satellite communication system is a good candidate to apply this technology. Despite the advantage, the cells using the same frequency should be placed far enough to avoid interference problems. Adjacent beams should use different frequencies. This means that the same frequency is used at least two cells apart from each other. Since the two cells are placed far away from each other, it will not cause any interference problems.

The frequency reuse technique is accomplished by low side lobe level performance in the beam pattern. Based on this idea, we are using a 7 frequency reuse scheme, which means that the neighbouring beams do not use the same frequency. In order to evaluate the interference problems, we need to check the side lobe levels at the cells with the same frequency. Using beam 1 and beam 14 as an example, Figure 7-25 illustrates the idea of the frequency reuse technique for beam 1 and beam 14. The inner '×' and '◦' smaller circles are the coverage area for beam 1 and 14, respectively. The question is to find the maximum sidelobe level outside the outer big circle for each beam. That means to find the interference level for the two cells with the same frequency. For beam No.1, the maximum sidelobe outside the big red circle should not be larger than a certain threshold, especially the sidelobe level inside the coverage area of beam 14, in order to suppress the interferences. This is also true for beam 14.

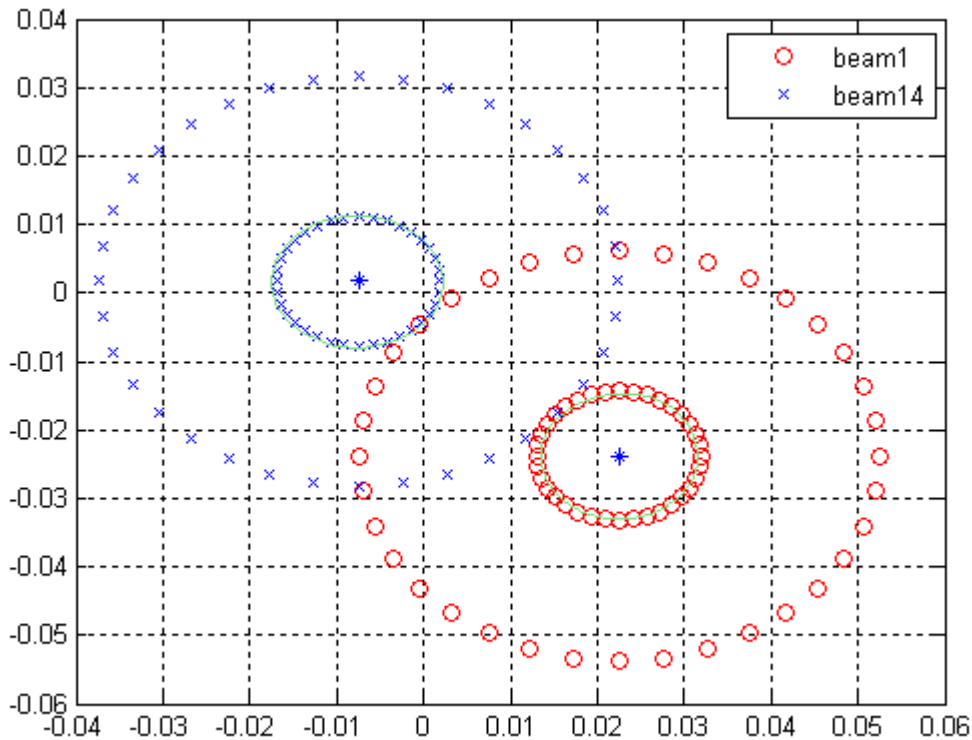


**Figure 7- 25 Frequency reuse for beam 1 and 14**

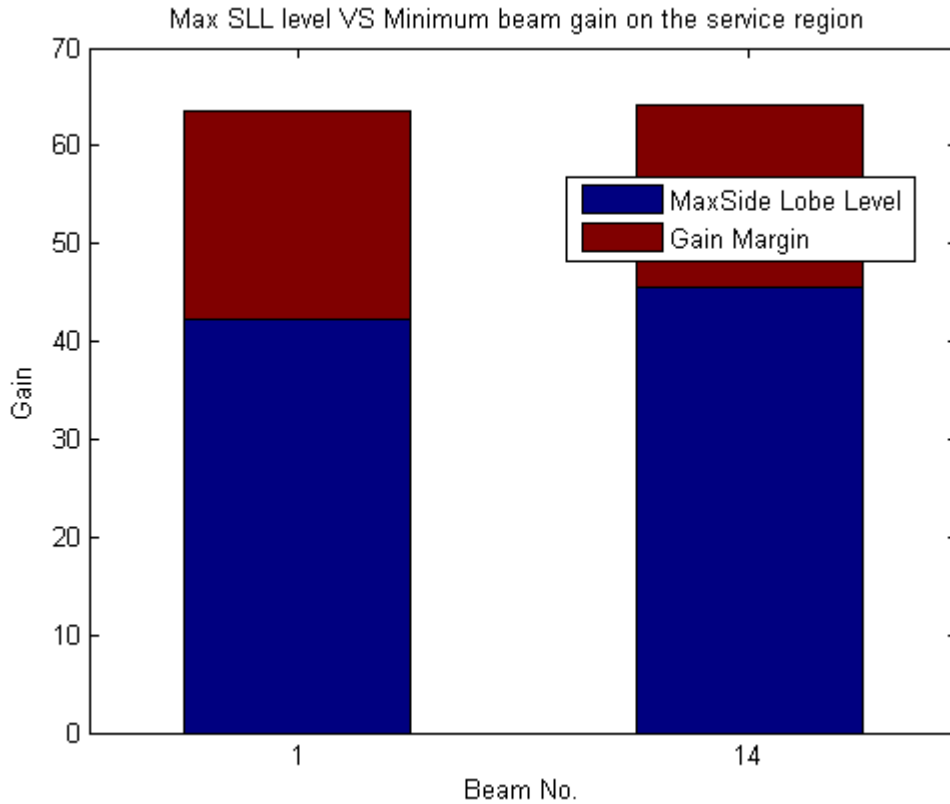
### 7.5.1 Test Methodology

In the first place, we need to test the sidelobe level of beams 1 and 14 outside the big circle as shown in Figure 7-25 for the error free case. Then the interference level at the two beams will be calculated. This will be the reference level. The working frequency is 2180 MHz.

Then, the same test will be carried for beams 1 and 14 with error vectors. Then, the results can be compared with the reference level in attempt to find the influence of the error vectors to the sidelobe levels.

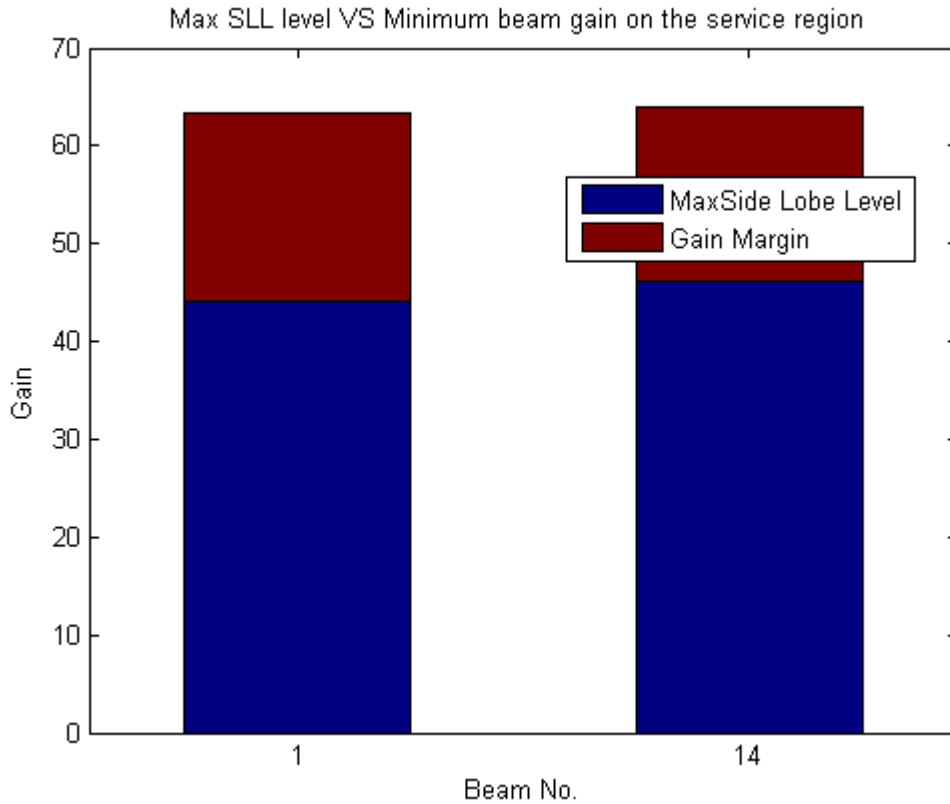
### 7.5.2 Simulation Results

Figure 7-26 shows the simulation results for the error free case. The horizontal axis is the beam number and the vertical axis is the minimum beam gain at the coverage edge for each beam. The blue bars show the sidelobe levels and the dark red bars show the gain margins for each beam. Take the bar on the left as an example, this bar shows that the minimum gain at beam 1's coverage edge is 63.6dB and the maximum sidelobe from beam 14 is 42.3 dB. Thus, we can see that the gain margin is 21.3 dB in this case. Then, reading the right bar, we see the minimum gain at the beam 14 coverage edge is 64.2dB and the gain margin is 18.6 dB. From this figure, we can see that the sidelobe for beam 1 is larger than that of beam 14 and its minimum edge gain is lower than that of beam 14. The reason is that beam 14 is located quite near the focal point of the reflector and beam 1 is an edge beam. This results in a worse beam shape compared to that of beam 14.



**Figure 7- 26 SLL for error free case**

Next, we can investigate the influence of the error vectors on the side lobe levels. We will omit the simulation results for individual components and jump to the case where all the components are added with error vectors. First, let us see the results from -20 dB reflection coefficients with 2 dB standard deviations and 0 dB mean value for the transmission coefficients amplitude error with 0.1 dB standard deviations. The transmission coefficients phase error is 2 degrees.



**Figure 7- 27 SLL for  $S_{ii\_errorMean} = -20\text{dB}$ ,  $S_{ii\_errorSTD} = 2\text{dB}$  and  $S_{ij\_errorSTD} = 0.1\text{dB}$ ,  $S_{ij\_errorPhase\_STD} = 2\text{ degrees}$**

Figure 7-27 shows that the gain margin for beam 1 and beam 14 decreased to 19.3 dB and 17.96 dB, respectively. The error vectors have some negative impacts on the side lobe level performance, but not too much. As we discussed before, in case of beam coverage edge gain variation performance, the system could tolerate that the reflection coefficients' amplitude error mean value is -20 dB with 2 dB deviations and that the transmission coefficients' amplitude standard deviation is 0.2dB with 5 degrees phase errors. We also check the side lobe performance in this case.

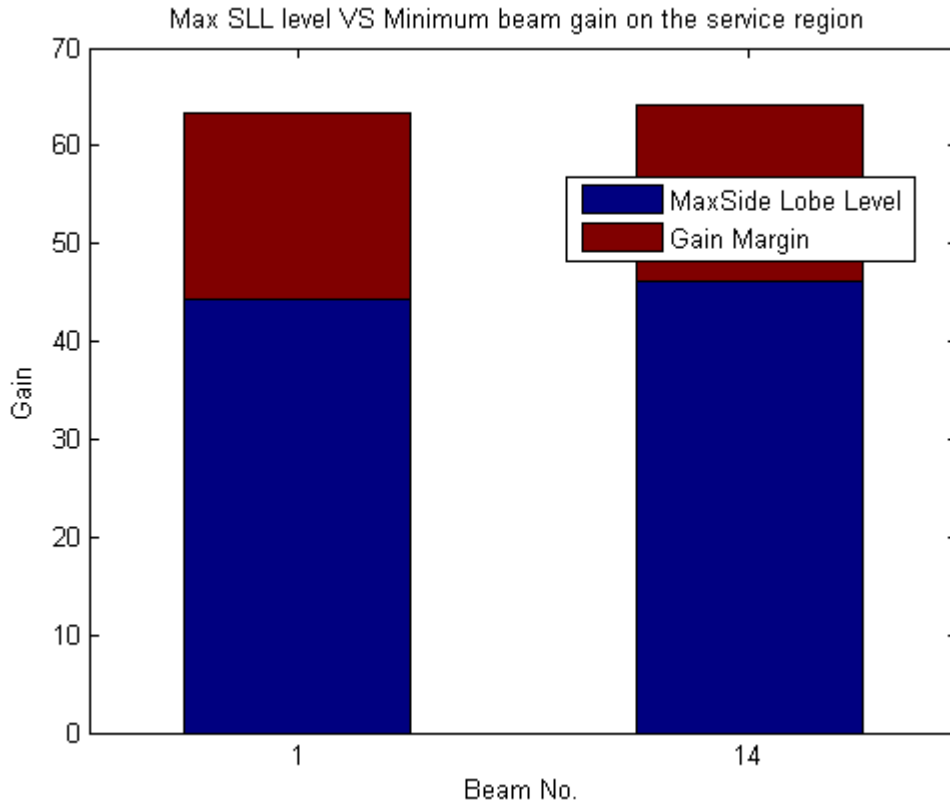


**Figure 7- 28 SLL for  $S_{ii\_errorMean} = -20\text{dB}$ ,  $S_{ii\_errorSTD} = 2\text{dB}$  and  $S_{ij\_errorSTD} = 0.2\text{dB}$ ,  $S_{ij\_errorPhase\_STD} = 5\text{ degrees}$**

Figure 7-28 shows that the side lobe levels increased a little bit which results in the gain margin being reduced to 18.9dB and 17.8dB respectively. As the error vectors are random, sometimes we will obtain even worse results. Normally, the gain margin should be larger than 20 dB. But in our system, we can see that it is hard to achieve this goal. If we need better results, side lobe performance optimization of the nominal element excitation coefficients for each beam should be added.

## 8 Conclusions and Future Work

A Matlab model for the mobile satellite communication system has been built and tested. This model is applied for an array of 42 antenna feeds which can generate 22 beams simultaneously. The model can easily be extended to an even larger array with more beams. A simple model, which is used to illustrate the beamforming algorithms, was constructed in Simulink as well.

The onboard transmitter and receiver systems have been modelled. The two separated systems were combined with diplexers. The LNA performance of the receiver system is quite important and the efficient utilization of the onboard transmit power is of great interest. The noise performance of a receiver was calculated and the carrier to noise ratio was obtained. The tolerances for each component are specified and the isolation level between the receive and transmit system are defined. In order to avoid the third order inter-modulation interference problem, more than 100 dB isolation between the transmitter and receiver networks is needed. During the modelling stage, different design topologies were compared, such as different types of beamforming networks, different transmitter network design schemes, the layout of the beamforming network and the HMPA, the choice of Butler matrix and so on.

The gain variations on the beam coverage edge show acceptable results, but the side lobe level performance can hardly reach the -20 dB requirement. The single stage results show that the beamforming network is quite sensitive to amplitude and phase errors. Thus this component should be more accurate than other components. The left hand Butler matrix can accept more error tolerances due to working at low power levels. But the HPAs and the right hand Butler matrix need to be more accurate than the left hand Butler matrix.

The future work can be to investigate optimization of the sidelobe performance and the beamforming network structure. Different error vector distributions can be added in the system as well. In the model used here, we just assumed that the error vectors are normal distributed. They could be modelled by other distributions such as the truncated normal distribution or the square root cosine distribution. By adding these different error vectors, we can compare the system performance from different angles. In addition, measured data for different components can also be placed in the model and tested. Here, we only used measured data of the antenna patterns and the diplexers.

## References

- [1]. Denno, S.; Ohira, T., “Modified Constant Modulus Algorithm for Digital Signal Processing Adaptive Antennas With Microwave Analog Beamforming”, IEEE Transactions on Antennas and Propagation, Vol 50, Jun 2002
- [2]. Ohira, T.; Suzuki, Y.; Ogawa, H.; Kamitsuna, K. ,“Megalithic microwave signal processing for phased-array beamforming and steering,” IEEE Trans. Microwave Theory Tech., vol. 45, pp. 2324–2332, 1997.
- [3]. www.mathwork.com
- [4]. John Litva, Titus Kwok-Yeung Lo, “Digital Beamforming in Wireless Communications”, Artech House, London, 1996.
- [5]. Robert E. Collin, “Foundation for Microwave Engineering”, 2<sup>nd</sup>, McGraw-Hill, Inc, 1992.
- [6]. P. Gabellini, N. Gatti, “Advanced Optimization techniques for satellite Multi-beam and reconfigurable antenna and payload systems”, 29<sup>th</sup> ESA workshop, 2007.
- [7]. Wilkinson, E.J.; “An N-Way Hybrid Power Divider”, IRE Transactions on Microwave Theory and Techniques, Volume: 8 , Issue: 1, pp116-118.
- [8]. L. I. PARAD; R. L. MOYNIHAN, “ Split-Tee Power Divider”, IEEE Transactions on Microwave Theory and Techniques, Vol 13, pp.91-95, 1965
- [9]. Timothy Pratt; Charles Bostian; Jeremy Allnutt, “Satellite Communication”, 2<sup>nd</sup>, John Wiley & Sons, 2003
- [10]. Son H. Huynh; Antony Ho; C. Harry Chen, “A septet Beam Forming Network for Reflector Multiple Beam Antennas”, TRW Space and Electronics, 1997.
- [11]. Tom Y. Otoshi, Noise Temperature Theory and Applications for Deep Space Communications Antenna Systems, Artech House, London, 2008.
- [12]. C. K. S. Miller; W. C. Daywitt; M. G. Arthur, “Noise Standards, Measurements, and Receiver Noise Definitions”, IEEE, Vol.55, No.6, 1967, pp865-877.
- [13]. John Zacharatos; Robert B. Williamson, “ Power Versatile Satellite transmitter”, U.S Patent 4907004, 1990
- [14]. Per Magnusson; Niklas Kurlberg, “A Compact Rx/Tx Dual Circular Polarization Satellite Antenna Array Element Including Diplexers”, Berlin, EuCAP 2009
- [15]. Thomas A. Milligan, "Modern antenna design", McGraw-Hill, cop., New York, 1985.
- [16]. Kerry W. Spring; Harry J. Moody, “ Divided LLBFN/HMPA transmitted architecture ”, U.S Patent 4901085, 1990
- [17]. Mallon, K.P., “TWTAs for Satellite communications: Past, present and future”, IEEE International Vacuum Electronics Conference, pp14-15, 2008.
- [18]. R. Belanger; N. Taylor; E. Bertenyi, and C. Kittiver, “MSAT communication payload system overview”, 15<sup>th</sup> AIAA International Communications Satellite System Conference, Part 1, AIAA-94-0981-CP, Feb. 1994